UPTAKE OF ELLIPSOIDAL POLYSTYRENE NANOPARTICLES IN HUMAN MESENCHYMAL STEM CELLS

Laura Victoria Flórez

Submitted to the Biological Sciences Department
in Partial Fulfillment of the Requirements for the Degree of
Bachelor in Biology

Director
Professor Doctor Katharina Landfester
PhD. Physical Chemistry
Director Physical Chemistry of Polymers Research Group
Max Planck Institute for Polymer Research

Codirector
Professor Carlos Jaramillo Henao
M.Sc. Microbiology
Professor Department of Biological Sciences
Universidad de Los Andes

Contents

1. SUMMARY

The promising applications of nanoparticles in biological research have made them a matter of great interest in recent years. The fact that these can be easily internalized by different types of cells make them a valuable tool for cell labeling and selection, tracking of specific molecules, gene therapy and drug delivery, among others. In addition to size, material and surface chemistry, it has been suggested that particle shape can be important for their internalization in cells. In order to assess such hypothesis, the first phase of the present study was dedicated to the production and characterization of fluorescent ellipsoidal polystyrene nanoparticles generated by stretching spherical particles embedded in a polyvinylalcohol film. During the second phase of the study, the influence of ellipsoidal shape in comparison to spherical shape on particle uptake by human mesenchymal stem cells was evaluated. It was observed that ellipsoid particles are taken up to a lesser extent than control spherical particles for different uptake time periods (1, 4, 8, 20 and 48 h) and particle concentrations (9.4, 18.8, 37.5, 75, 150 and 300 µg/mL). Also, none of the particles showed toxicity in the tested conditions. Observations regarding particle shape are in accordance to the idea that ellipsoid particles with an unfavorable orientation in relation to the cell membrane are not easily internalized and in consequence, the overall uptake is reduced. Furthermore, it was found that the treatment to which the particles are submitted in order to be transformed into ellipsoids results in higher particle uptake. The presence of surfactant, free sodium styrene sulfonate (comonomer) and/or its homopolymer in the untreated dispersion is considered the direct or indirect cause of this outcome. The obtained results contribute in understanding the role of shape in particle uptake. This is useful, for example, in studies using biological models or in biomedical applications. Moreover, these observations can play a role in describing particular aspects of particle-cell interactions.

RESUMEN

Las potenciales aplicaciones de las nanopartículas en estudios biológicos han hecho de estas un tema de gran interés en años recientes. Partículas en este rango de tamaño son fácilmente internalizadas por diferentes tipos de células y por ende, constituyen una valiosa herramienta en marcaje y selección de células, rastreo de moléculas específicas, terapia génica y transporte de fármacos, entre otros. Además del tamaño, material y química de la superficie, se ha sugerido que la forma de las partículas puede ser relevante en la toma por parte de células. Con el fin de evaluar dicha hipótesis, la primera fase del presente estudio se dedicó a la producción y caracterización de nanopartículas de poliestireno elipsoidales y fluorescentes, generadas mediante el estiramiento de partículas esféricas embebidas en una película de polivinilalcohol. Durante la segunda fase del estudio se evaluó la influencia de la forma elipsoidal en comparación a la forma esférica para la toma de partículas por parte de células madre de mesénquima humana. Se observó que las partículas elipsoidales fueron tomadas en una cantidad menor que las esféricas para diferentes tiempos de incubación con partículas (1, 4, 8, 20 y 48 h) y diferentes concentraciones de partículas (9.4, 18.8, 37.5, 75, 150 y 300 µg/mL). Ninguna de las partículas evaluadas presentó toxicidad en las condiciones analizadas. Las observaciones respecto a la forma corresponden a lo esperado, considerando que las partículas con orientación desfavorable respecto a la membrana celular no serán fácilmente internalizadas y por lo tanto, la cantidad total de partículas tomadas será menor. Adicionalmente, se observó que el tratamiento aplicado para convertir las partículas en elipsoides resulta en mayor toma por parte de las células. La presencia de surfactante, sulfonato de sodio de estireno (comonómero) y/o el homopolímero correspondiente en la dispersión sin tratar se ha considerado la causa directa o indirecta de esta diferencia. Los resultados obtenidos contribuyen a entender el rol de la forma para la toma de partículas en células. Esto sería útil, por ejemplo, en estudios que empleen modelos biológicos o en aplicaciones biomédicas. Adicionalmente, estas observaciones pueden servir para describir aspectos particulares de la interacción partícula-célula.

2. INTRODUCTION

The integration of nanotechnology in biological disciplines has been a matter of great interest in the past few years. Ongoing research on this subject has given origin to a wide variety of inquiries and promising applications such as cell labeling and selection, targeted drug delivery, differentiation of stem cells [1], DNA uptake [6], immunization and detoxification [7]. The term nanoparticle refers to structures with sizes that range between a few nanometers and some hundred nanometers. They are therefore a couple of orders of magnitude smaller than cells although larger than single molecules. In fact, it has been observed that a wide variety of cells are able to take up materials specifically in the range of 50 - 200 nm [1, 7, 8]. Particularly useful properties are available within this size range, such as a high surface area and the possibility to incorporate reporters or contrast agents that could be effectively delivered by means of nanoparticle uptake into cells [1].

A significant majority of the research on interaction between cells and nanoparticles has been carried out using spherical particles composed of different materials and surface characteristics [1, 2, 7-9]. There is, however, a growing interest on exploring shape as influential factor in particle uptake [9-12]. Variation in surface area and dependence on orientation of anisotropic particles during interaction with cells might offer interesting insights on uptake mechanisms and efficiency. Moreover, shape plays a role in particle degradation, targeting and transport of particles at both extracellular (velocity, diffusion, adhesion) and intracellular levels (internalization and sorting) [3]. There is still, nonetheless, a lack of research on comprehensively describing the effect of particle shape on interaction with cells [3]. In this context, a model to further investigate this inquiry is proposed, which offers advantages such as: i) a fairly simple and properly standardized method for particle synthesis, employing the versatility of polymeric materials and possibility of particle labeling; ii) application at the nanoscale, which is similar to that of biological molecules (e.g. proteins, DNA) and structures (e.g. viruses and some bacteria) [10] and is already observed to be a favored size range for internalization [1, 8]; iii) the use of human mesenchymal stem cells (MSCs), which are a promising tool in current biomedical research. This project will thus investigate the uptake of anisotropic (ellipsoid) polystyrene nanoparticles in MSCs in comparison to spherical particles of the same volume, surface and composition characteristics. The aim of this approach is to give first steps on understanding the role of anisotropy in nanoparticle uptake and thus contribute in the elucidation of relevant aspects of cell-nanoparticle interaction.

3. BACKGROUND

3.1   POLYMERIC NANOPARTICLES

3.1.1 Synthesis via miniemulsion polymerization

Among the various techniques to generate polymer dispersions, emulsion polymerization is commonly and broadly applied. It is also possible to generate polymer dispersions by means of microemulsions, suspension polymerization or the generation of secondary dispersions by precipitation or solvent assisted emulsification. Nonetheless, these methods present several disadvantages. The emulsion polymerization, for example, is restricted to radical homopolimerization of water-soluble monomers. Microemulsions require excessive use of surfactant, whereas the other mentioned techniques can present insufficient colloidal stability [13]. Under this perspective, the so called miniemulsion polymerization is an advantageous and highly versatile method among other polymerization strategies, being capable of producing complex polymeric nanoparticles that are well suited for biological applications [1, 2]. Significant advantages of this technique are the ability to adjust particle size (obtaining relatively narrow particle size distributions), to incorporate a fluorescent dye for further visualization [2, 8, 14] and to minimize kinetic and stability complications present in other polymerization techniques [13, 15].

As for all heterophase polymerization processes, the miniemulsion method is defined not by a size range, but by how it operates. The system required to carry out a classic miniemulsion polymerization consists of an oil-in-water emulsion containing an oil-soluble monomer, a hydrophobe stabilizing agent, an initiator and a surfactant. It is also possible to polymerize a water soluble monomer via the so called "inverse miniemulsion" using a water-in-oil system. In this project only particles synthesized by direct miniemulsion were employed. Such process is carried out as follows: initially, the droplets in the heterogenous fluid must be mechanically disrupted, increasing the surface area of the emulsion. Subsequently, a high force dispersion method like ultrasonication (in the case of reduced quantities) is used for homogenization (Fig. 1). In order to obtain a stable system, two effects must be controlled: (i) Ostwald ripening (degradation caused by molecular diffusion) and (ii) coalescence by collisions. The first of these phenomena comprises a thermodynamically-driven spontaneous process in which molecules from small droplets diffuse towards larger droplets. Such effect arises from the greater Laplace pressure of small droplets that creates a net mass flux by diffusion [13]. In other words, the energetically unfavorable surface molecules in small droplets tend to incorporate in larger droplets, where a lower surface area to volume proportion is acquired. Small droplets will then easily disappear and an increase in the average droplet size results. In
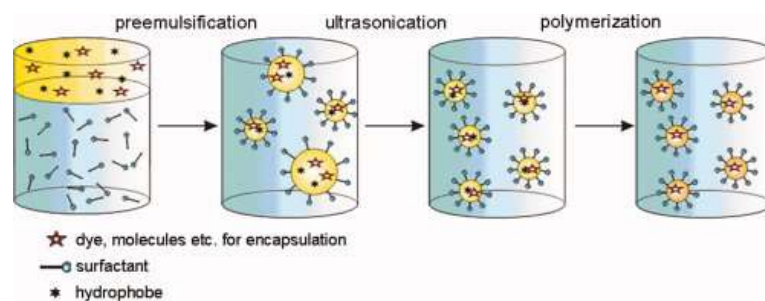

Figure 1. Principle of miniemulsion polymerization [2].

order to surpass such outcome, a stabilizing molecule that is insoluble in the continuous phase and highly soluble in the dispersed phase (in this case an ultrahydrophobe) is added. Its function is to reduce the vapor pressure as defined by Raoult's Law. In these circumstances, when molecules from a small droplet diffuse to a larger droplet the small droplet will have an osmotically reduced vapor pressure in comparison to the large one. The compensation of this difference will then avoid the disappearance of the small droplet, what results in an average size that may vary between 50 and 500 nm depending on the amount and type of surfactant. Coalescence by collisions, the second undesired effect, is controlled by the use of appropriate surfactants [13].

Due to the fact that polymerization initiates and proceeds independently in each droplet without significant interaction or exchange kinetics, the miniemulsion system comprises a set of so called "nanoreactors" working in a parallel fashion [13]. Such scenario offers important advantages regarding control of the process, as well as versatility and tuning possibilities for the desired product characteristics.

3.1.2 Applications in Biology and Biomedicine

Polymeric nanoparticles are useful in a wide range of areas, being suitable research models and with high potential in practical applications [1, 2, 14-19]. There is a growing interest on exploiting this technology for biological uses taking advantage of their high colloidal stability, chemical resistance and the facility to produce them in comparison to other nanoparticulate systems like liposomes or micelles [2]. Thus, cellular uptake of polymeric nanoparticles and the possibility to use them as carriers for specific molecules has been extensively investigated in recent years. Transfection agents have been used in model studies to modify particle surface and in this way enhance uptake. Surface modification is also possible using antibodies or ligands, which can be useful for targeted drug or gene delivery by means of a defined interaction with antigens or receptors on the cell surface [2, 20]. Furthermore, incorporation of tracer molecules like fluorescent dyes offers multiple possibilities such as cell labeling and selection [1, 2, 21], tracking of specific molecules or studying the uptake process and fate of the particles at an intracellular level [7]. Nanoparticles can also be promising tools for non-viral vaccination, immunoassays, immunodiagnostics and controlled drug release [2, 21, 22].

It is noteworthy that the incorporation of specific molecules in the nanoparticles can also protect these from being removed from the cell cytoplasm or from suffering enzymatic or hydrolytic degradation [2, 3]. In a similar manner, nanoparticles can be advantageous in the design of efficient bioreactive systems where usually limited stability of antibodies or enzymes can be a major drawback. This is the case for several biosensing or separation and purification processes in which affinity reaction steps take part. So called "molecular imprinting" on polymeric nanospheres is then a convenient tool for the design of artificial receptor-like binding sites that are useful in biological research and applications [18].

As to biomedical applications, even challenges in regenerative medicine or implementation of new routes for drug administration can find advantages in nanoparticles [1]. For example, previous studies in neurobiology have shown that a major difficulty in effective drug transport into the central nervous system is to cross the blood-brain barrier. This is a compact layer of endothelial cells, through which only low molecular weight compounds can cross by passive diffusion and reach the brain. Regarding larger molecules, only those that are recognized as essential for the brain metabolism can cross the barrier. As

reported by Landfester *et al.* [2], recent studies show advances on the application of certain types of polymeric nanoparticles that can effectively permeate the blood brain barrier and therefore offer meaningful perspectives in brain therapeutics.

Nanoparticles carrying magnetite as a marker are another good example of their potential biological applications. These can be employed for cell separation, magnetic resonance imaging [1, 2], magnetically controlled drug delivery and even immobilization, purification and isolation of nucleic acids [2].

Regarding immunological topics there is significant progress in nanoparticle-based labeling systems for immunoassays since these exhibit increased specificity and affinity. The possibility to achieve high concentrations of label units and binding sites in nanoparticles are in essence responsible for these convenient properties [23]. Under a different perspective, Azzi *et al*. [24] demonstrated the ability of polylactide particles carrying cyclosporine A (an immunosuppressing agent) to inhibit T-cell proliferation and production of inflammatory cytokines. This targeted immunosuppression was possible by selectively delivering the nanoparticles to the lymph nodes, highlighting once more the advantages of nanoparticles for directed transport of molecules into cells.

As mentioned above, gene delivery techniques based on nanoparticles is a promising application as well. Gene therapy involves introduction of exogenous genes in specific cells with purposes such as replacement of absent or defective genes and immunotherapy against cancer or viral infections. It is also considered useful in tissue engineering, since the introduction of specific genes (e.g. sequences encoding growth factors) can enhance local tissue repair. However, delivery of naked DNA has complications since it can be rapidly degraded by nucleases *in vivo*, showing only transient gene expression [20, 25]. It is thus of great value to develop efficient carrier systems that can overcome these difficulties and offer further advantages. In this sense, being susceptible to endocytosis and having the possibility to manipulate their target is highly desirable [25]. Although viral vectors have been used in this area and show high transfection efficiency, they have several drawbacks for *in vivo* applications. These present fast elimination from the circulatory system, limited size capacity for carrying genetic material, toxic risks and possible undesired immune reactions as well as the possibility of malignant transformation. Alternatively, nanoparticles do not have the former disadvantages and are quite versatile [20]. Polymeric nanospheres have already been used in drug delivery using biodegradable materials. Regarding nucleic acid (DNA or RNA) delivery, both entrapping mechanisms and surface binding systems have been addressed. In the later case, the anionic character of nucleic acids enables ionic interaction with a cationic polymer [25]. Various promising applications in this area have been reported, such as successful sustained delivery of plasmid DNA (pDNA) [26, 27] as well as small interfering RNA (siRNA) using biocompatible nanocarriers [28, 29]. An interesting case is the study of Patil & Panyam achieving effective *in vitro* silencing of a model gene, fire fly luciferase, with PLGA (poly (D,L-lactide-*co*glycolide) - PEI (polyethylenimine) nanocapsules as a siRNA delivery system [28]. Regarding pDNA, it has been observed that plasmid encapsulation in biocompatible and biodegradable polymeric materials is appropriate to accomplish gene delivery and even higher expression levels than naked DNA. Furthermore, evidence of sustained release after several weeks can be achieved when using the nanocapsules as delivery system [27]. These are just a few examples of the growing number of studies which take advantage of nanoparticles to efficiently transport nucleic acids

into cells. This is consistent with the value that molecular biology techniques represent for a broad variety of useful approaches, emphasizing on the versatility of nanoparticles as tools in biological sciences.

3.1.3 Particle characteristics relevant to uptake in cells

Having an overview of the multiple applications that polymeric nanoparticles can offer and understanding the benefits of the miniemulsion technique to produce particles for biological purposes, it is essential to comment on the factors that are decisive for interaction with cells.

3.1.3.1 Material: type of polymer

The type of polymer composing nanoparticles not only has an influence on the level of particle uptake by different cell lines [1, 22] but also determines the specific applications of each type of particle. The degree of hydrophobicity of the polymer can have an effect on protein adsorption in the culture medium prior to uptake by cells and therefore modify the particle-cell interaction. Also, the glass temperature and/or the degree of crystallization of different polymeric materials determines the mechanical properties of the particles, including their softness at cell culture conditions [22]. Several studies have shown clear differences in cellular uptake for polymers such as polyisoprene, poly-(methyl methacrylate), poly-(L-lactide) [1], or even among the same monomer family varying the side chain type and length [22].

Biocompatibility and biodegradability of the polymeric material are also essential for practical applications of nanoparticles. Examples of such materials are poly (alkylcyanoacrylate)s [1], polyanhydrides, polyamides, polyphosphazenes and specially a well described variety of polyesters such as poly (Ɛ-caprolactone), poly (lactic acid), poly (glycolic acid) and their copolymer poly (lactic acid-*co*-glycolic acid) [3]. Experiments with nanoparticles composed of these polymers have been reported, aiming towards the development of systems for sustained release of pharmacologically active substances [1, 3].

Although polystyrene (PS) does not easily degrade in cellular environments, this material has been extensively used in many studies on nanoparticle uptake by cells [22] and was the principal component of the particles used in the present study (except one, which is specifically indicated). It is relatively easy to emulsify and polymerize styrene by means of radical polymerization using the miniemulsion technique [2], through which desired particle characteristics can be tuned. Furthermore, surface functionalization can be acquired by copolymerization of styrene with other specific monomers. The non-biodegradability and possible accumulation of PS makes it inappropriate for direct applications in human studies. Nonetheless, it can be a useful model for long-term experiments in cell cultures [1], interactions with biomolecules, cell labeling and a wide variety of *in vitro* biological studies.
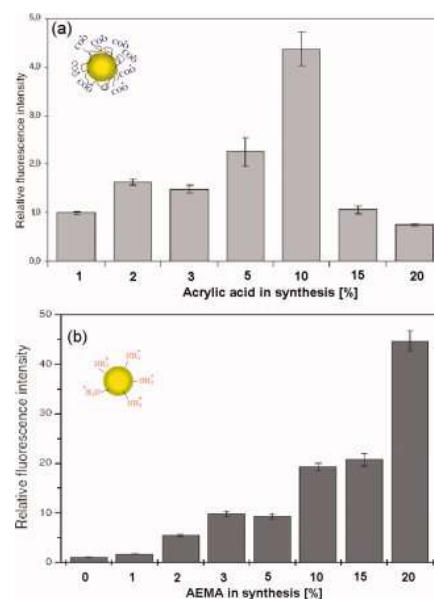
3.1.3.2 Surface chemistry

Surface characteristics of nanoparticles are crucial for their uptake by different cell lines. The direct interaction of the particle surface with the cell membrane can be determinant for the mechanism and thus amount and rate of uptake [1, 2, 6-8, 14, 21, 22]. Functionalization with covalently bonded charged groups present in a specific comonomer has made it possible to describe the response of several cell types to cationic (e.g. amino) and anionic (e.g. carboxylic, phosphonate) [1, 2, 7, 8, 14, 21] groups on particles. Both positively and negatively charged particles are usually preferred in comparison to non-charged, as reported in several studies [2, 8] (Fig. 2). Particles with a positive charge show the highest uptake signals due to the net negative charge of the cell membrane. Moreover, increasing the number of charged groups on the particles generates a higher uptake by the evaluated cells. In the case of acrylic acid (AA) as a comonomer (which provides carboxyl, negative groups) this effect is inverted after a certain amount of charged groups (corresponding to 10 wt% of AA relative to styrene) (Fig. 3) [2, 21]. Further studies on this area have also shown that the mechanisms involved in the uptake of positively or negatively charged nanoparticles is different and might vary according to the cell line [8] (see section 3.3.1). Other modifications of the surface are possible by using different surfactants, amino acids, antibodies or nucleic acids [22].
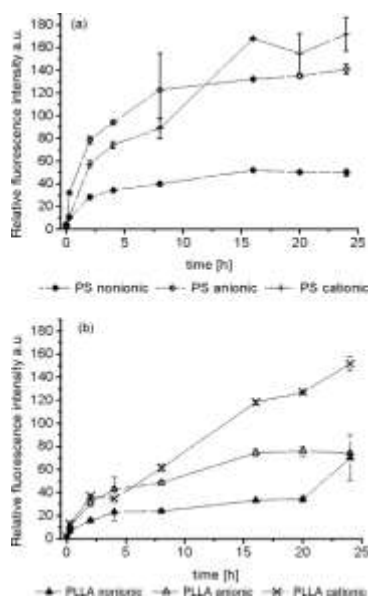
Figure 2. Uptake kinetics of non-charged, cationic and anionic PS (a) and PLLA (b) nanoparticles in HeLa cells [2].

Figure 3. Uptake in HeLa cells of particles with different amounts of functional comonomer (a) carboxyl (-) ; (b) amino (+) [2].

3.1.3.3 Geometry: size and shape

Along with particle surface chemistry, size has been extensively studied as an influential factor in cellular uptake [1-5, 30]. Polymeric particles in the submicrometer range are currently used for biological applications [2] and have been broadly investigated. It has been observed that hydrodynamic diameters between 50 and 200 nm are particularly favorable for uptake by a variety of cell lines like MSCs and HeLa [1] and also, that the internalization rate is affected by size [5]. In the biomedical area studies show that only particles up to 100-300 nm in diameter can passively cross the tumor endothelial barrier through fenestrations, which is an important fact for drug delivery and tumor targeting purposes [5]. Alternatively, microspheres larger than 40 µm in diameter can have applications as embolizing agents (i.e. occlusion of blood vessels) [30].

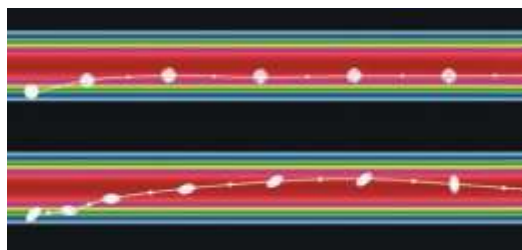It is known that particle size can be decisive for the uptake mechanism. Larger particles (>1 µm) tend to be internalized primarily by phagocytosis, while smaller ones can be taken up by different mechanisms (e.g. receptor mediated endocytosis, pinocytosis or nonspecific endocytosis) [4, 8]

As it might be expected, in most studies related to particle geometry radius has been the principle parameter to consider, especially because a great majority of research on nanoparticle uptake in cells and other biological applications has been done with spheres [3, 9]. Nonetheless, other factors such as surface area and orientation, which are also related to shape, can be directly responsible for important aspects of particle-cell interaction. This is hence a valid reason to pursue a more comprehensive picture of the relevant characteristics in particle geometry by including shape as an essential feature.

3.2 ANISOTROPIC PARTICLES

3.2.1 Role of particle shape in biological applications: previous studies

It is already known that size is highly influential in many particle functions, not only during direct interaction with cells for internalization. Shape can also be crucial in such processes as previously described in the literature. For instance, experiments on degradation of spherical nanoparticles demonstrated the significance of diameter as well as surface area, which are dictated by shape [3]. For drug delivery purposes, efficient transport of particles in the body must consider velocity and diffusion parameters, as well as adhesion to walls in blood

Figure 4. Trajectory model of neutrally buoyant spherical and ellipsoidal particles in an idealized capillary (straight cylindrical tube) under typical capillary hydrodynamic conditions [5].

vessels, airways and intestines. It is highly desirable in vascular targeting to accumulate particles in close proximity to the blood vessel walls (termed *margination* in physiology) since this enables sensing of specific markers or fenestrations through which they can access smaller vessels. Analyzing hydrodynamic factors of spherical and non-spherical particles moving in a linear laminar flow, it has been predicted that in contrast to ellipsoids, spheres will not undergo lateral drifts unless an additional external force is applied. Non-spherical particles, on the other hand, have a more complex motion pattern that can be useful to control their margination dynamics. These show lateral drifting with a direct dependency on aspect ratio and tend to mobilize from one side of the capillary to the other. Ellipsoids are thus able to "explore the vessel" (Fig. 4). Such predictions were also supported by *in vitro* experiments [5].

Considering targeting ability, surface area available for targeting ligands can have great importance. Also local curvatures might affect ligand interactions, opsonin[1] adsorption and the degree to which particles fit the contours of target cell membranes [3]. In fact, a more thorough study of the scenario has determined that for each particle shape there is a specific size for which the probability of adhesion presents a maximum. This depends on a combination of two effects: hydrodynamic forces and area of interaction.

---

[1] Opsonin refers to any of various proteins (as complement or antibodies) that bind to foreign particles and microorganisms (as bacteria) making them more susceptible to the action of phagocytes.

The optimal condition is to avoid significantly strong hydrodynamic forces (the case of a large particle) but still attain a sufficient area of interaction and possible adhesion [5].
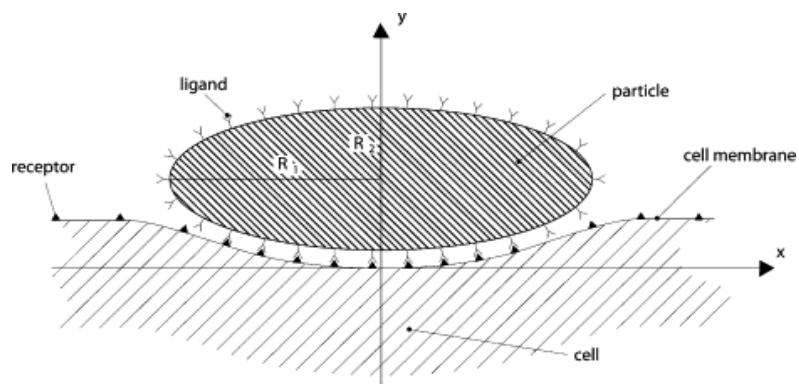
Figure 5. An ellipsoidal particle laying with long axis parallel to the cell membrane [4].

As to internalization, particle orientation can be determinant in the case of anisotropic particles [4, 5, 9]. Champion and Mitragotri have observed such effect at the micrometer level evaluating the uptake of different anisotropic PS particles in alveolar rat macrophage cells. Elongated particles laying with their long axis parallel to the cell membrane (Fig. 5) have an internalization rate that tends to zero [4, 5]. It was concluded that at the point of first contact between particle and cell membrane, shape, not size, decisively determines whether cells will proceed with phagocytosis or simply spread on the particle. Size alone basically limits the completion of phagocytosis when the target volume is larger than the macrophage volume [9]. Under a similar perspective, these same authors investigated the shape effect by synthesizing elongated worm-like polystyrene particles, whose phagocytosis rates were found to be strongly reduced in comparison to spherical particles. It is suggested that curvature points on the particle are preferred for internalization and therefore, reducing high curvature spots to two end points prevents uptake by phagocytes. This is in fact a desirable result when the purpose is to avoid phagocytic uptake of a carrier previous to its arrival near the target cell [31].

A few studies at the nanometer size range were also reported. Chithrani *et al*. investigated the intracellular uptake of different sized (14 to 100 nm) and shaped colloidal gold nanoparticles. Comparing spherical vs. rod-shaped particles, the first of these show a higher uptake by HeLa cells. Several reasons are mentioned in order to explain the results: i) surface area in contact with the cellular membrane reduces number of available receptors, ii) higher amount of surfactant on rods and iii) non homogenous adsorption of serum proteins from cellular culture medium on rods causes weaker ligand interactions [10].
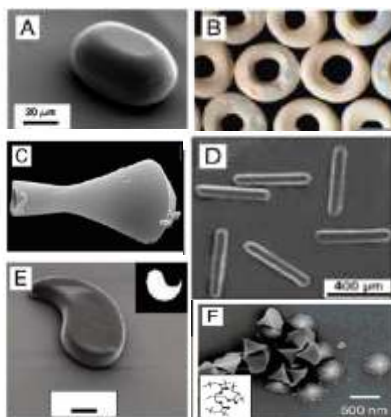
Regarding the internalization process during receptor-mediated endocytosis (until now the best described mechanism for nanoparticle uptake [32, 33], see section 3.3.1), Decuzzi & Ferrari have developed a model to describe and analyze the effect of particle shape and size considering energetic factors of ligand bonding as well as cell membrane and cytoskeleton deformation. Previous studies had already shown that there is a critical radius for cylindrical and spherical particles under which receptor-mediated endocytosis is energetically unfavorable. This also depends, however, on the density and affinity of ligand-receptor bonds and the flexibility of the cell membrane. Furthermore, the authors have suggested that if sufficiently large ligand densities are generated at rims with small curvature, particles should be internalized regardless of their orientation at the contact spot with the cell membrane [4].

It is worth to mention that shape could also have an effect on intracellular transport and sorting of particles. After they are internalized, particles are found encapsulated in vesicles (i.e. endosomes,

lysosomes or phagosomes) and can be transported for further processing [3]. Although the fate of particles depends on several other factors that are not yet described in detail, it could also be meaningful to consider the role of shape at this stage.

3.2.2   Fabrication methods

Several years ago it was still a big challenge to obtain non-spherical particles of well-defined shapes, which are also narrowly distributed in terms of size. The synthesis of microparticles in the range between 10 nm and 1000 µm is clearly dominated by spherical systems since minimization of interfacial energy leads to such geometry [34]. During the past decade, however, interesting approaches have been explored for acquiring anisotropic particle latexes of desirable characteristics. These could be appropriate in a broad range of applications such as response to external fields, rheological (fluidic systems) studies and biological models or practical uses [3, 34, 35]. Two categories among anisotropic particle preparation methods have been described: i) *ab initio* approaches and ii) manipulation of pre-formed spherical particles. The first category includes lithography, microfluidics and photopolymerization techniques, which are usually more demanding in terms of equipment but offer the possibility to produce a wider variety of shapes with a precise morphology (Fig. 6) [3]. In the present study, however, a manipulation technique was used. These can be simpler than the former, but offer a more reduced range of shape possibilities. Starting with spherical particles it is possible to modify shape by means of self-assembly, template assisted self-assembly [3] or film stretching [3, 35]. In this last case, spherical particle latex is embedded in a polymer film and stretched at a temperature above the glass transition of both the matrix and particle materials. It is possible then to generate ellipsoid particles of different aspect ratios that can be previously determined [3, 35, 36]. Additionally, stretching in two dimensions results in disk-shaped particles [9].

Figure 6. Anisotropic particles produced by *ab initio* methods [3].

Concerning biological applications, the method used should meet certain requirements in order to obtain particles of suitable characteristics [3]. First of all it should be able to work with the appropriate polymers for intracellular delivery or the desired purpose. In addition, it should allow the incorporation and/or permanence of the chosen molecules (i.e. proteins, DNA, therapeutic drugs) without inactivation of their functions. Finally, it is important that the method does not inhibit post-production processing and that it allows satisfactory scalability possibilities [3].
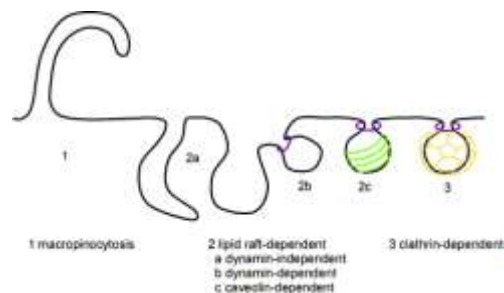
3.3 PARTICLE UPTAKE BY CELLS

3.3.1   Uptake mechanisms

Understanding the specific mechanism of particle uptake by different cell types is of great relevance for exploiting biological applications of nanoparticles. Although there is evidence that nanoparticles are able to enter cells through encapsulation in membrane vesicles, a thorough description of the specific routes is still in progress. Several possible mechanisms (i.e. pinocytosis, non-specific endocytosis, receptor-

mediated endocytosis and phagocytosis) might be involved depending on the specific particle and cell types [1, 7, 8].

As previously mentioned, different uptake mechanisms operate for different particle sizes. Above 1 µm, phagocytosis and macropinocytosis are the major internalization strategies involving a substantial rearrangement of cytoskeletal structures [5, 33]. On the other hand, smaller particles with diameters below 500 nm are usually taken up by receptor mediated endocytosis, pinocytosis or nonspecific endocytosis [1]. In between 500 nm and 1 µm it is suggested that a

Figure 7. Representation of endocytosis mechanisms [1].

"mixed mode" operates [5]. In any case it is possible that more than one mechanism takes part for the same type of particles [8].

There is still a lot to learn on endocytosis routes. However, several pathways have been investigated in various biologically active molecules and viruses [1, 8] and the process of functional compartmentalization of the plasma membrane has been described to some extent. The well-known clathrin dependent pathway is among these the best characterized until now [32, 33]. It involves a protein "basket-like" assembly coating the formed compartments or pits [8], which are usually 100 to 500 nm in size [4]. A second type of pathways is regulated by lipids and lipid-protein interactions, where the term "lipid rafts" becomes relevant. These are highly ordered microdomains formed due to the interaction of sphingolipids² and sterols [33]. Pits formed from lipid rafts during endocytosis can be uncoated or coated by protein (caveolin), depending on the specific machinery involved. Invaginations coated with caveolin are refered to as caveolae and are typically 50-60 nm in size [4]. Regions rich in clathrin and lipid rafts can have a high concentration of receptors that can trigger internalization when these bind to external ligands. In this manner, receptor-mediated endocytosis turns out to be the most effective internalization mechanism for both natural (e.g. enveloped viruses) and artificial particles [4]. The described routes are illustrated in figure 7. Furthermore, it is known that the surface charge of the particle and cell line also have an effect on the prevailing mechanism [8].

3.3.2   Human Mesenchymal Stem Cells (MSC)

The mechanism and conditions of particle uptake may vary significantly according to the cell type involved. Among the different cells in which nanoparticle uptake has been described are human mesenchymal stem cells (MSC) [1, 7, 14, 20, 37-41]. These are of particular interest due to their high proliferation and differentiation potential, which makes them a promising tool in regenerative medicine [1, 7, 14].

MSCs are a stem cell population present in adult bone marrow, which can replicate *in vivo* and *in vitro* as undifferentiated cells and have the potential of further differentiation in specific mesenchymal cell lineages (i.e. chondrocytes, adipocytes, osteocytes) [38, 41] (Fig. 8). They are also capable of expressing phenotypic characteristics of endoderm (endothelial cells), exoderm (neural cells) and other mesodermal

---

² Sphingolipids are a class of lipids derived from the aliphatic amino alcohol sphingosine. These compounds play important roles in signal transmission and cell recognition.

cell types like smooth muscle, skeletal myoblasts and cardiac myocyte cells. Found in a variety of tissues, adult stem cells participate in adult growth as well as repair and regeneration of damaged tissue. They also trigger such processes since they are capable of supplying growth factors and cytokines to repairing tissue [41].

MSCs present several advantages as a model system for studies on cell therapeutics and other biological inquiries. They are relatively easy to isolate, have a high expansion potential and are genetically stable. Furthermore, they have shown reproducible characteristics among different isolates and even different research groups or laboratories. MSCs are also compatible with tissue engineering principles. This cell type has already been tested in animal models for studies in cardiac treatments and their application in humans is in progress [41]. They clearly represent a promising tool in gene delivery for clinical therapy as well as in research on stem cell differentiation with a variety of applications [40].
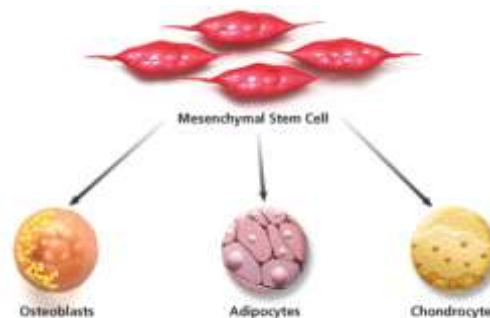
Figure 8. Mesenchymal Stem Cell (MSC) pathway. www.sigmaaldrich.com

## 3.4 TRACKING PARTICLES: FLUORESCENT DYES

In order to track particles both in extra- and intracellular environments it is useful to label these with fluorescent dyes. One of the possible methods for this purpose is physical adsorption of the dye on the particle surface. This has nevertheless disadvantages regarding instability and desorption. Alternatively, the miniemulsion process described in this study offers the possibility to embed a fluorescent dye in the polymeric particle during synthesis without any diffusion problems. Moreover, a comonomer with fluorescent properties can be included in the synthesis and this way particles with covalently bonded labeling molecules are obtained [1, 2, 21]. It is noteworthy that each organic fluorescent dye presents a defined excitation and emission spectrum. This is relevant in terms of suitability to the available analysis methods.

Four different dyes were tested in this study in order to obtain particles with suitable characteristics in terms of fluorescence permanence, dispersion stability, final product quantity and traceability after cellular uptake. A brief description of these dyes is presented below.

3.4.1 Perylene dyes

a) N-(2,6-diisopropylphenyl)perylene-3,4-dicarbonacidimide) (PMI).

Perylene diimides are known to be chemically and photochemically stable [42], generally inexpensive and have therefore a variety of applications (i.e. light-harvesting systems, organic electronic systems, fluorescent solar collectors) [43]. Furthermore, PMI (Fig. 9) has proved to be effective for polymer nanoparticle labeling [1, 2], having excitation and emission maxima at 479 and 539 nm respectively. It is incorporated in the particles due to the enclosure of the molecules in the hydrophobic polymeric shell formed during the synthesis process by miniemulsion [1].
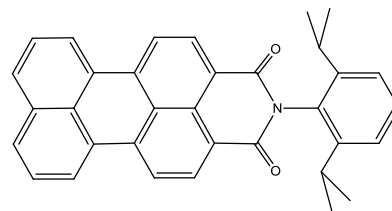
Figure 9. Chemical structure of N-(2,6-diisopropylphenyl)perylene-3,4-dicarbonacidimide (PMI).

b) Polymerizable perylene dye "N1" (Department of Synthetic Chemistry, MPIP).

Similar in structure to PMI, dye "N1" (Fig. 10) presents an extra aromatic ring with a free vinyl group. It is expected to copolymerize with the main monomer (styrene in the present study), in order to acquire fluorescent nanoparticles. N1 presents an excitation maximum at 500 nm and an emission maximum at 550 nm.
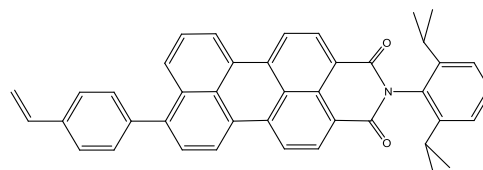
Figure 10. Chemical structure of the polymerizable dye "N1" (Department of Synthetic Chemistry, MPIP).

3.4.2 Boron-dipyrromethene (Bodipy) dyes.

This type of dyes has gained popularity in the past couple of decades because of their versatility and advantageous characteristics such as high fluorescent quantum yields and excellent chemical and photochemical stability. Moreover, they are known to be resistant towards aggregation in solution [44]. In this study two dyes of this family were evaluated (Fig. 11), which are both expected to polymerize with styrene. Bodipy 1 has excitation and emission maxima at 526 and 536 nm respectively, while Bodipy 2 presents maxima at 504 and 514 nm.
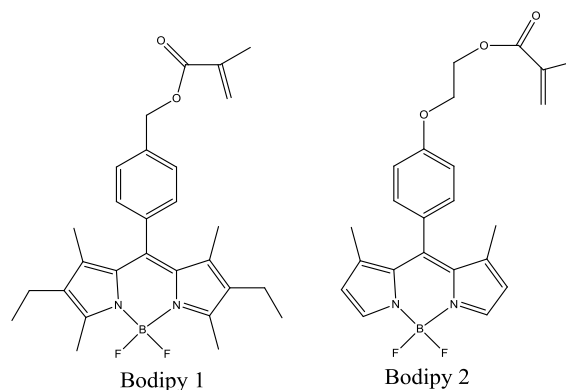
Bodipy 1   Bodipy 2

Figure 11. Chemical structure of boron-dipyrromethene (Bodipy 1 and 2) dyes (synthesized by Andrey Turshatov, Physical Chemistry Department, MPIP).

4. EXPERIMENTAL DESIGN

4.1 Objectives
General:
Investigate the effect of shape (ellipsoidal vs. spherical) in the uptake of polymeric nanoparticles in human mesenchymal stem cells.

Specific:
1. Synthesis of charged, fluorescent, polystyrene ellipsoid nanoparticles with composition and label characteristics appropriate for further cell uptake and the associated quantitative-qualitative analysis.
   1.a To optimize the stretching and recovery procedure in order to attain appropriate dispersion stability and particle quantities.
   1.b To characterize the ellipsoid and control (spherical) particles in terms of fluorescence, charge and diameter or aspect ratio.
2. Assessment of cellular uptake.
   2.a. To evaluate the toxicity of the ellipsoid nanoparticles synthesized by the described method.
   2.b. To carry out qualitative observations of particle-cell interaction comparing ellipsoids and spheres by means of microscopy.
   2.c. Quantitatively compare the uptake of ellipsoid and spherical nanoparticles by means of flow cytometry.

4.2 Hypotheses - Predictions
a. It is predicted that there will be no difference in cell toxicity between ellipsoid and spherical particles. It is considered possible, though, to find an effect of residue materials present without treatment (surfactant and remaining components of the synthesis) or after the stretching process (i.e. PVA residues).
b. Particle orientation will play a role in ellipsoid uptake by MSCs: it is expected to observe preferential uptake of particles which establish contact perpendicular to their major axis in comparison to ellipsoids that are parallel to the cell membrane.
c. Overall uptake of ellipsoid particles will be quantitatively lower than uptake of spherical particles, considering that part of the ellipsoidal particle population will lay with the long axis parallel to the cell surface.

5. MATERIALS AND METHODS

5.1 Production of fluorescent ellipsoidal nanoparticles
Ten different polymeric spherical nanoparticles synthesized by the miniemulsion polymerization process [45] were tested and five of them used for the fluorescence analysis and generation of anisotropic (ellipsoid) particles (Table 1). The remaining five were not redispersable in water after the stretching and cleaning procedure and therefore not further used. The corresponding monomer, functionalization type and relevant characteristics of each type of these particles are presented in Appendix 1. For experiments

on particle uptake by cells, polystyrene particles originally labeled CH266 and synthesized by PhD. Student Christoph Hauser were used (Department of Physical Chemistry, MPIP). The corresponding components as used for the synthesis are presented in Table 2.

Table 1. Particles used for fluorescence analysis and generation of anisotropic (ellipsoid) nanoparticles.

LABEL	ORIGINAL DISPERSION	MONOMER	SURFACE FUNCT. (Comonomer)[1]	FLUORESCENT DYE	λ_{Ex}	λ_{Em}	DYE (%)[1]	HYDRODYNAMIC DIAMETER (nm)	STRETCHING /HEATING METHOD[2]
LF-K2	DC63	styrene	-	PMI	490	540	0.05	390	a
LF-K5	AM-NSC-N1	styrene	$-NH_3^+$ (AEMH, 5%)	N1	500	550	0.07	164	a
LF-K6	CH237	methyl methacrylate	-	Bodipy 1	526	536	1	124	a
LF-K8	CH266	styrene	$-SO_3^-$ (SS, 3%)	Bodipy 2	504	514	0.5	125	b
LF-K9	CH257-2	styrene	-	Bodipy 2	504	514	0.5	140	b

1. wt % relative to monomer.
2. (a): manual stretching in oil bath; (b): stretching in oven. See section 5.1.1.

Table 2. Miniemulsion composition for the synthesis of sulfonated polystyrene fluorescent particles CH266.

Component	Function	Weight (g)
V59	Oil-soluble initiator	0.1
Styrene	Monomer	5.819
Hexadecane	Hydrophobic stabilizing agent	0.259
SDS	Ionic surfactant	0.02983
Sodium styrene sulfonate	Comonomer	0.18025
Bodipy 2	Polymerizable fluorescent dye	0.02988

5.1.1 Particle stretching

The materials used for film formation and particle recovery were poly (vinyl alcohol) (polyvinyl alcohol 40-88 from Aldrich Chemistry, degree of hydrolysis 86.7-88.7 mol%, degree of polymerization 4200, M_w 205 000, residual acetyl content 10.0-11.6%) and 2-propanol (Aldrich Chemistry). Formerly spherical nanoparticles were transformed into ellipsoids following two different variants of the method described by Ho *et al.* [35] and modified by PhD student Christine Herrmann (Department of Physical Chemistry, MPIP). The first step of both variants of the process consists on the formation of poly (vinyl alcohol) (PVA) (3.5 wt% PVA in water solution) films containing the latex of the spherical nanoparticles at a concentration of 8 or 10 wt% in relation to PVA (Appendix 1). The film is then dried and mechanically stretched to a previously determined draw-ratio (final length of twice the original length of the film, i.e. aspect ratio = length/width = 4) at a temperature above the glass transition point (T_g) of both PVA (matrix) and PS (particles). In the first variant used, small films were manually stretched in a metallic frame and in the second, medium sized films were stretched in a computer-controlled stretching device. For each variant of the process the specific conditions and further steps were:

a. **Manual stretching in oil bath:** 4 g of PVA/water solution were mixed with the corresponding amount of particle latex (according to the solid content) and stirred at 700 rpm during 2 to 3 h for homogenization. The PVA solution containing the particle latex was then placed on a flat glass surface (8 cm in diameter) and left overnight to dry. Films were cut obtaining a 4 x 3.5 cm piece which was then submerged for 5 s in a 140 °C oil bath and manually lengthened. A metallic frame (model proposed by Ho *et al.* [35] (Fig. 12)) was used for such purpose. The removal of oil traces on the film was done by soaking in pure isopropanol and stirring for 2 hours (repeated 3 times with fresh isopropanol).

b. **Stretching in oven:** 24 g of PVA/water solution were mixed with the corresponding amount of particle latex (according to the solid content) and stirred at 700 rpm during 2 to 3 h for homogenization. The PVA solution containing the particle latex was then placed on a polystyrene rectangular dish (12 x 8 x 0.1 cm) and left approximately 72 h until dry. Films were cut in 12 x 4 cm pieces, approximately 0.05 mm thick. Each piece was then fixed to mechanical clamps inside an oven previously heated to 140 °C and submitted to controlled stretching up to the desired length (twice the original effective length, ignoring the area covered by the clamps; i. e. from 8 to 16 cm) at a speed of 300 mm/s.
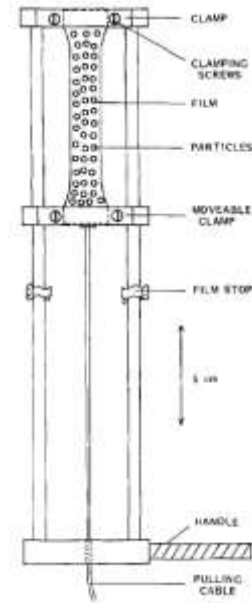
Figure 12. Schematic illustration of frame designed by Ho *et al.* for film stretching (Not to scale) [3].

As a control, in both cases a second film of the same concentration and containing the same latex was submitted to the entire procedure (including 140 °C) excluding only the stretching step (Fig. 13; num.2).
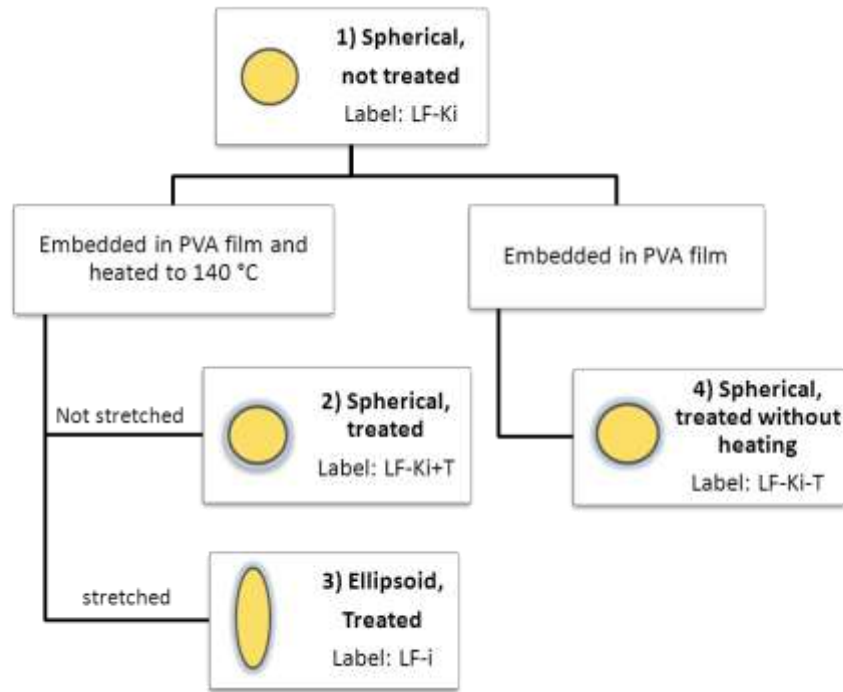
Figure 13. Scheme of the 4 resulting particles depending on treatment variation. i = sample number in labeling system applied for each sample after treatment (see Table 1 for sample description).

5.1.2 Particle recovery

After cooling at room temperature, the borders of the film that are not homogenously stretched were discarded. In order to determine which the appropriate homogenous region of the film was, a test film was marked with grid lines (0.5 x 0.5 cm). After stretching, rectangles of the desired dimensions (1 x 0.25 cm, corresponding to a 100 % draw ratio) were used as reference to delimit the area where particles are uniformly stretched. Further observations with scanning electron microscopy were carried out to support these results. The central area of the film (7 x 0.8 cm, established as previously mentioned) was weighed and cut into small pieces, which were dissolved overnight in 5 mL of a 3:7 (volume relation) isopropanol:water solution. For some of the samples a heating step up to 70 °C during 1 hour was included, based on the protocols suggested by Ho *et al.* and Madivala *et al.* [35, 36], in order to completely dissolve the PVA matrix. The cases and reasons why this step was modified are discussed further. As a cleaning procedure and for removal of PVA, each sample was then centrifuged 3 times (14000 rpm, 90 min) redispersing in fresh isopropanol/water solution each time. Subsequently, ellipsoid particles were redispersed in water and solid content was calculated by freeze drying.

5.1.3 Fluorescence

Fluorescence intensity was measured by duplicate using a TECAN Plate Reader infinite® M1000 (monochromator). In the case of particle dispersions 75 µg/mL particle concentration (and 150 µg/mL when specified) was used. Fluorescence Correlation Spectroscopy was performed by Dr. Kaloian Koynov (Physics of Polymers Department, MPIP). Measurements were done on dispersions with 0.035 wt% particle concentration using a commercial FCS setup (Zeiss, Germany) consisting of the module ConfoCor 2 and an inverted microscope model Axiovert 200. A Zeiss C-Apochromat 40×/1.2 W water immersion objective was employed. The fluorophores were excited by an Argon laser at λ = 488 nm and a LP505 emission filter was used. For detection, avalanche photodiodes were used to enable single-photon counting. An eight-well, polystyrene-chambered coverglass (Laboratory-Tek, Nalgene® Nunc International) was used as sample cell. The calibration of the observation volume was done using Rh6G (hydrodynamic radius of 0.8 nm). Further specifications regarding the autocorrelation function employed are described in [46]. UV/Vis absorption from 300 until 780 nm was measured in a PerkinElmer Lambda 25 Spectrometer.

a) Particle dispersions. Four different particle dispersions were analyzed (LF-K2, LF-K5, LF-K6, LF-K8) corresponding to different dye types and particle material (Table 1). Four different treatments were applied for fluorescence evaluation corresponding to the complete film stretching and cleaning procedure, the same process omitting heating and/or stretching steps, or no treatment at all (Fig. 13). The applied excitation and emission wavelengths are indicated in Table 1.

b) *PMI in solution.* PMI solutions in 1-Octanol with concentrations of 56 and 207 µg/mL were placed in small glass containers and submerged in a 140 °C oil bath for a defined period of time (0, 25 or 60 s). Fluorescence intensity was subsequently measured. Excitation and emission wavelengths applied were 490 and 540 nm respectively.

c) *Bodipy 2 - PS Particles in solution.* Thermal stability of Bodipy 2 dye in polystyrene particles (CH257-2, Table 1) in toluene solution was evaluated. The probe solution with a concentration of 0.7 mg/mL of formerly freeze-dried sample was kept for 5 minutes in an oven previously heated to 140°C. No film or stretching procedure was carried out in this case and the control probes were also handled at a

concentration of 0.7 mg/mL. The UV/Vis spectrum was subsequently evaluated and compared to control solutions of the same concentration. Fluorescence intensity was measured as well.

5.1.4 Characterization

5.1.4.1 Size

The hydrodynamic radius of the original spherical particles was measured by means of Dynamic Light Scattering (DLS) with a Submicron Particle Sizer NICOMP[TM] 380. Additionally, particle size was measured on Scanning Electron Microscopy images (200 particles per sample were measured and averaged) using the MeasureIT 5.1 Olympus Software. This method was also employed for anisotropic particles, measuring both axes in order to calculate their aspect ratio (length/width).

5.1.4.2 Charge and functionalization

12 mL of a 3% solid content fraction of the CH266 dispersion were dialyzed in cellulose dialysis tubing Visking typ 20/32 (Carl Roth GmbH, Germany), previously submerged in distilled water for 30 minutes. The sample was placed in 1.6 L distilled water and dialyzed during a total period of 140.5 h. Samples (1 mL) were taken after 17, 26.5, 41, 50.5, 65, 91 and 119 h during the process and the wash water was changed eleven times. After the mentioned 140.5 h the conductivity of the wash water showed no change when compared to a water sample stored in the beginning of the corresponding dialysis step and therefore, the process was considered completed. Conductivity values were acquired using a LF413T measuring cell in a ProLab2000 Digital Multi-meter (Schott Instruments), at room temperature (20-25 °C).

a)   Particle Charge Detector (PCD)

The numbers of charges per gram of polymer, per particle and per surface area were measured in dialyzed and not dialyzed CH266 samples. Each measurement was carried out 3 times in a Mütek PCD-02 Particle Charge Detector using a standard automatic titrator (702 SM Titrino, Metrohm). Samples were previously diluted to a concentration of 0.001 g/mL and polyelectrolyte poly(DADMAC) of the same concentration was used.

b)   Inductively Coupled Plasma Spectroscopy (ICP) and Nuclear Magnetic Resonance (NMR)

Sulfur content was measured in an Activa HORIBA Jovin Yvon CCD-ICP-OES spectrometer. The solid content of each of the 7 samples taken during the dialysis process as well as the initial non-dialyzed and final dialyzed CH266 was calculated by freeze drying. 3 mL of each dispersion was then diluted to 0.8 wt% to carry out ICP measurements. ^{1}H-NMR was measured in DMSO (Methyl sulfoxide-d_6, 99.5 + atom % D, Aldrich Chemistry) and Chloroform (99.8 + atom % D, Aldrich Chemistry) solutions in a 300 MHz Bruker Avance II console.

5.2 Cell uptake experiments

5.2.1 Cells.

Human mesenchymal stem cells (MSCs) were provided by collaborators in the Institute of Clinical Transfusion Medicine and Immunogenetics at the University of Ulm, Germany. The cells were generated from bone marrow aspirations or explanted hips, as described in [41], after obtaining informed consent. MSCs were kept in α-MEM medium (Bio Whittaker TM) supplemented with 20% Fetal Bovine Serum, 1% Penicillin-Streptomycin, 1% Sodium-Pyruvate and Ciprobay (2 mg/mL). Cells were grown in a humidified

incubator at 37 °C and 5% CO_2 in triple flasks. Cell seeding and preparation protocols varied according to the specific analysis method as described in the following sections.

5.2.2. Fluorescence activated cell sorting.

A quantitative analysis of the effectively incorporated particles and their toxicity level was carried out using a fluorescent activated cell sorter (FACS, Partec CyFlow® ML desktop Flow Cytometer). Cells were seeded in 12-well polystyrene plates at a density of 25,000 cells/cm^2, in 1 mL of cell culture medium. On the next day, the medium volume was readjusted to 0.5 mL per well and particle dispersions were added at the desired concentration. These were kept in a humidified incubator at 37 °C and 5% CO_2, allowing particle uptake for 20 h (otherwise indicated). After such period, cell culture medium in each probe was collected; each well was washed with 0.5 mL of PBS Buffer (Calcium free) (Gibco, Germany) and the adhered cells were trypsinized with 0.3 mL of a 0.5% Trypsin (Gibco, Germany) in PBS solution. Cells were centrifuged during 3 minutes at 15000 rpm and the pellet resuspended in 0.3 mL PBS. The cell suspensions were incubated with 20 µL of 28.6 mg/mL 7-actinomycin (7AAD), which is a dye that permits the differentiation of dead, early apoptotic and living cells. The cells were submitted to a last centrifugation (3 min at 2000 rpm) and resuspension step (in 1 mL PBS) in order to carry out the FACS measurement. The 488 nm blue laser was used to analyze particle uptake (excitation of fluorescent dye in particles, Bodipy 2) and the 561 nm yellow laser to analyze toxicity (excitation of 7AAD dye). The fluorescence signals obtained were normalized according to the fluorescence intensity measured by FCS (Table 3) to obtain comparable uptake efficiencies.

In order to evaluate the effect of PVA remaining in solution or on the surface of treated particles, an additional FACS experiment was carried out using the original CH266 (LFK8) previously dispersed in solutions of PVA (same as used for films) in water at different concentrations (15, 45, 90 and 135 µg/mL). This concentration range was determined based on the estimation of the amount of PVA residues if a 10 or 20 nm thick layer remains on the treated nanoparticles (29 and 44 µg/mL respectively). The layer thickness was approximated using DLS measurements presented in Table 5 (10 nm size difference) (section 6.1.3) and acquired from other particle dispersions that were also submitted to film treatment (20 nm size difference). Higher PVA values were also included in the range, considering that extra PVA could remain in solution and not only on the particle surface. LFK8 particles were left overnight in the PVA solutions as continuous phase and the next day added to the seeded MSCs as described previously for every other FACS cell uptake experiment. The amount of nanoparticles corresponded to a final concentration of 75 µg/mL (calculated according to the solid content of the original dispersion) available for cell uptake.

5.2.3 Microscopy.

5.2.3.1 Confocal laser scanning microscopy (CLSM)

CLSM was employed to confirm intracellular localization of the nanoparticles. MSCs were seeded in Ibidi µ-Slides VI$^{0.4}$ at a density of 2000 cells/cm^2 in 30 µL of culture medium per channel. After cell adhesion, an extra volume of 60 µL of culture medium was added. On the next day medium was removed and 100 µL of fresh medium containing the particle dispersion at a concentration of 75 or 150 µg/mL was added. After

20 h each channel was washed with 100 µL PBS Buffer (Gibco, Germany) and 100 µL of the staining solution were added. Images were acquired using Leica LAS AF software on a Leica SP5 II System with a DMI6000 CS Microscope body equipped with 5 lasers, a multiline argon with 458, 476, 488, 496, 514 nm, a DPSS 561nm Laser, a HeNe 494 nm, 633 nm Laser and a 592 nm CW STED Laser with a HCX PL APO CS 63×/1.4-0.6 oil lens (Leica, Germany). Staining with 2.5 µg/mL CellMask™ Orange (Molecular Probes, Germany) labeled the cell membrane red when excited by a 561nm laser and was detected at 575-600 nm. The cell nucleus was stained with 0.5 µL/mL Draq5™ (Biostatus Limited), which was excited by a 633 nm laser and detected at 650-700 nm. The Bodipy 2 dye used as label in the nanoparticles was excited by 488 nm laser light and detected at 500-550 nm. To avoid crosstalk between different dyes, emission signals were collected independently in serial mode. Images were taken with a pinhole size of 1 Airy Disk [a.u.] and a line average of two.

5.2.3.1 Electron Microscopy

Scanning Electron Microscopy (SEM) was used for qualitative observations of the nanoparticles on the cell surface, whereas Transmission Electron Microscopy was useful for intracellular recognition of the particles. MSCs were seeded in 24-well polystyrene plates at a density of 20,000 cells/cm^2 in 0.5 mL culture medium. Each well contained 3 or 4 Sapphire disks on which cells adhered. On the next day, particle dispersions were added at a concentration of 150 µg/mL and after a period of 4 or 20 h, sample preparation was carried out. Cells were fixed in 2.5% glutaraldehyde, postfixed in 2% aqueous osmium tetraoxide and dehydrated in graded series of Propanol. TEM samples were afterwards dried in a CPD 30 critical point drying apparatus and submitted to ultra-thin sectioning (80 nm) as a final step. TEM micrographs were taken in a Zeiss EM912. For SEM, samples were submitted to high pressure freezing and micrographs were taken in a 1530 Gemini LEO SEM (Zeiss, Germany) or in a Hitachi SU8000 SEM (Hitachi, Tokyo, Japan).

5.2.4 Statistical Analysis

After repeating three times FACS experiments at 75 and 150 µg/mL particle concentration and 20 h uptake using all three particle types and two replicas for each specific condition, quantitative results were normalized relative to the FACS fluorescence intensity value of control particles (spherical, not treated) at 75 µg/mL of each corresponding experiment and corrected according to the fluorescence intensity of the particles previously measured with FCS. The resulting data was analyzed by means of t-Student tests comparing spherical not treated vs. treated and spherical treated vs. ellipsoidal treated for 75 µg/mL and 150 µg/mL separately.

6. RESULTS AND DISCUSSION

## 6.1 Synthesis of fluorescent sulfonated ellipsoid nanoparticles

6.1.1 Fluorescence

For further analysis of cell uptake by Fluorescence Activated Cell Sorting (FACS) it was necessary to use fluorescently labeled particles that preserved fluorescence after the stretching procedure. The fluorescent dye should be able to maintain its properties after the 140 °C heating step and the washing process with isopropanol and water. Also, the fluorescent molecule should not affect the stability of the recovered particles on redispersion in water. Hence, different dye types (perylene and boron-dipyrromethene) were tested to optimize fluorescence intensity and stability in the final treated particles.

6.1.1.1 Perylene dyes

    a)   N-(2,6-diisopropylphenyl)perylene-3,4-dicarbonacidimide (PMI)

Fluorescence intensity appeared to be lost at a great extent after submitting PS-PMI particle dispersions (in film) to the high temperature step in oil bath (140 °C) (Fig. 14). Several hypotheses were proposed to explain these results: i) considerable error in solid content values due to the high uncertainty of mass determination for such a reduced amount of material; ii) Instability of the particle dispersions, which can cause inhomogeneous sampling for freeze drying; iii) Presence of poly (vinyl alcohol) residues on the particle surface, leading to variations in fluorescence, as well as in solid content determination; iv) dye aggregation, which can lead to effective fluorescence quenching [47] and could be favored at such conditions. To further investigate these observations, the fluorescence intensity of the dye in 1-octanol solution was measured before and after exposure to high temperature. The fluorescence intensity of PMI in solution was not altered after 25 or 60 seconds of submersion in a 140°C oil bath (Fig. 14). This result suggests dye stability at the temperature used for the stretching procedure and is also in accordance with the previously mentioned hypotheses, since agglomeration will not be favored in solution and the concentrations are not vulnerable to solid content error, presence of PVA residues or inhomogeneous sampling.
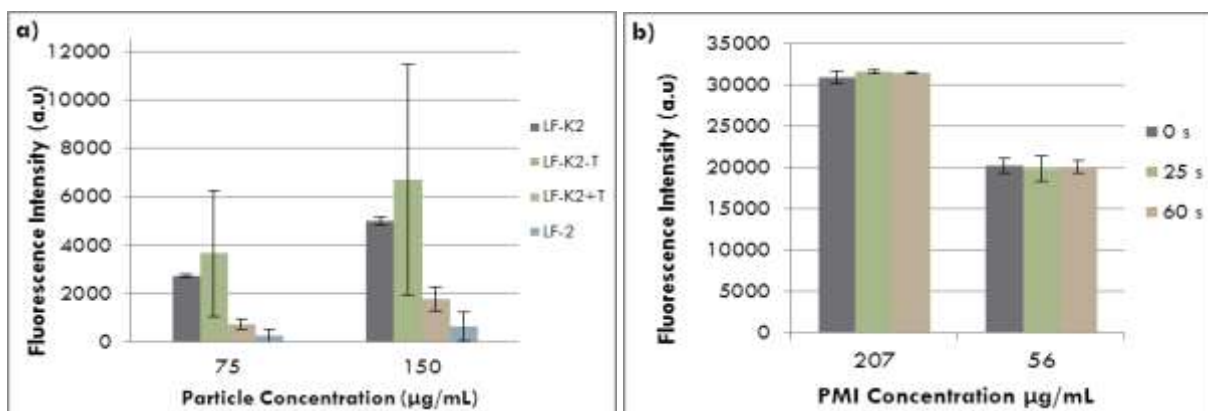
Figure 14. Analysis of PMI as fluorescent marker. a) Fluorescence Intensity of PS-PMI particle dispersions (see Table 1) submitted to the treatments described in fig. 13. Error bars correspond to solid content uncertainty and each measurement was done by duplicate. b) Fluorescence intensity of PMI in octanol solutions submitted to 140°C in an oil bath for 0, 25 and 60 seconds. Error bars correspond to standard deviation and each measurement was done by duplicate.

b) Polymerizable dye "N1"

A considerable reduction of fluorescence intensity was observed in the tested nanoparticles after temperature treatment (140°C oil bath) (Fig. 15). Qualitative observations suggested that this dispersion was not sufficiently stable after the recovery process. Therefore, it is highly probable that inhomogeneous sampling and significant error in solid content determination lead to the apparent fluorescence reduction. Further analysis of these samples (both with PMI and N1) using Fluorescence Correlation Spectroscopy (FCS) showed that in fact, the observed results were due to concentration error and inhomogeneity of the dispersions. It

Figure 15. Fluorescence Intensity of PS-N1 particle dispersions (Table 1) with a 75 µg/mL concentration submitted to the treatments described in Fig. 13. Error bars correspond to solid content uncertainty and each measurement was done by duplicate.

was not possible to obtain statistically reliable values due to the low amount of material. The relatively few particles encountered in treated samples using Fluorescence Microscopy appeared to conserve fluorescence. Nonetheless, not only fluorescent, but also stable and homogeneous dispersions are desirable. Therefore, the particles labeled with perylene dyes (both PMI and N1) were considered inappropriate for cell uptake experiments.

6.1.1.2 Bodipy dyes

Although fluorescence intensity appeared to be reduced with the heating and stretching procedure on the poly(methylmethacrylate)-Bodipy 1 particle dispersions (Fig. 16), these were also unstable and containing

a reduced amount of material. Such conditions resulted once more in high uncertainty values. Furthermore, PMMA and Bodipy 1 were observed to be less appropriate for observation with fluorescence microscopy than PS particles labeled with Bodipy 2 (LFK9, see Table 1). The second system was thus preferred and further evaluated as described in the subsequent experiments. The UV/Vis absorption spectrum of PS-Bodipy 2 particles dissolved in toluene showed no difference between the heated and not heated samples, confirming heat stability for the temperature applied in the stretching procedure (140°C). Fluorescence intensity measurements confirmed such result (Fig. 17).

Figure 16. Fluorescence Intensity of PMMA-Bodipy 1 particle dispersions Table 1) submitted to the treatments described in Fig. 13. Error bars correspond to solid content uncertainty and each measurement was done by duplicate.
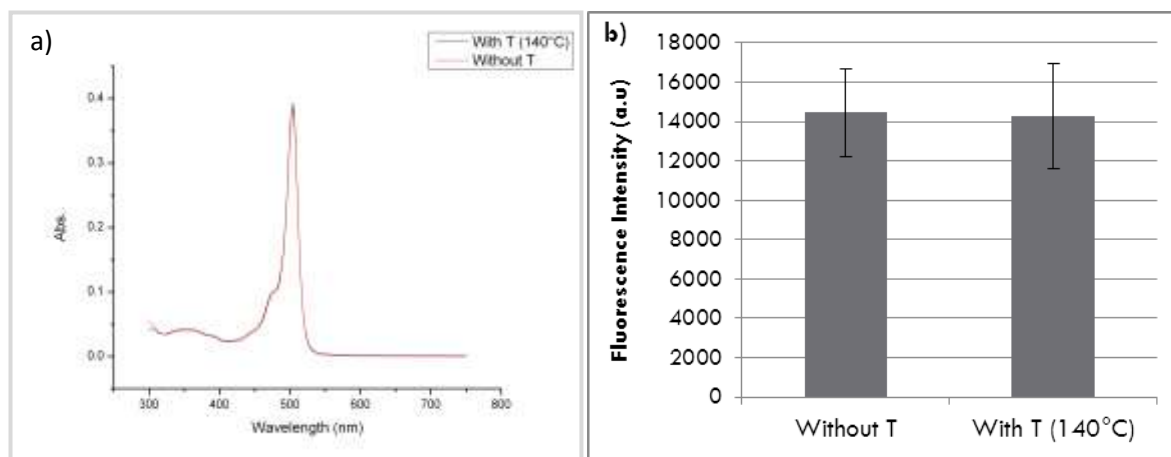
Figure 17. Analysis of Bodipy 2 as fluorescent marker in PS nanoparticles. a) UV/Vis Absorption spectrum of LFK9 (see Table 1) particles in toluene solution with and without heating (140°C). b) Fluorescence intensity of the same samples with and without heating (140°C). Error bars correspond to solid content uncertainty and each measurement was done by duplicate.

Subsequently, a second PS-Bodipy 2 particle dispersion was tested (LFK8, Table 1 and Appendix 1). These were functionalized with sulfonate groups from sodium styrene sulfonate (SSNa) as comonomer, which was included in the miniemulsion synthesis in order to acquire higher stability on the final redispersion in water. Fluorescence Correlation Spectroscopy (FCS) measurements on PS-(SO$_3^-$)-Bodipy 2 particle dispersions showed that fluorescence variation during the heating and stretching procedure was minor (Table 3). It is of high importance that these measurements were not susceptible to the former problematic factors regarding inexact solid content values. In agreement with the FCS results,

fluorescence intensity measured on the Plate Reader monochromator did not show significant differences among the three samples (Fig. 18). Having fulfilled the desired stability and fluorescence properties, PS-(SO$_3^-$)-Bodipy 2 particle dispersion (LFK8 formerly CH266, see Tables 1 and Appendix 1) and the corresponding treated particles (LFK8+T and LF8) were used for cell uptake experiments. LFK2 (formerly DC63, see Tables 1 and Appendix 1) were used for a set of additional electron microscopy analyses, which do not require the presence of a fluorescent marker.
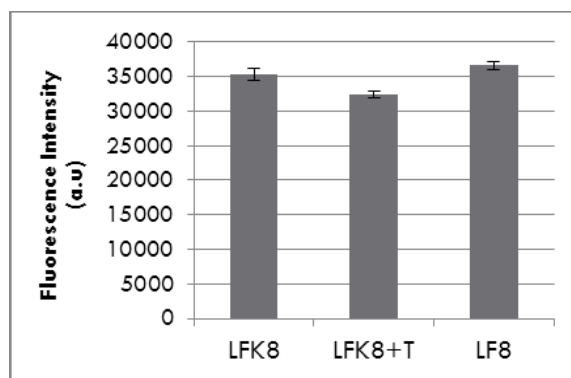
Figure 18. Fluorescence Intensity of PS-Bodipy 2 particle dispersions (see Table 1) submitted to the treatments described in Fig. 13. Error bars correspond to solid content uncertainty and each measurement was done by duplicate.

26

Table 3. Fluorescence intensity of PS-Bodipy 2 particle dispersions (see Table 1) submitted to the treatments described in Fig. 13 measured with Fluorescence Correlation Spectroscopy (FCS).

SAMPLE	Fluorescence per Particle (Counts/particle [kHz])	% Fluorescence (rel. to untreated)
LFK8	222 ± 33	100.0
LFK8+T	299 ± 45	134.7
LF8	209 ± 31	94.1
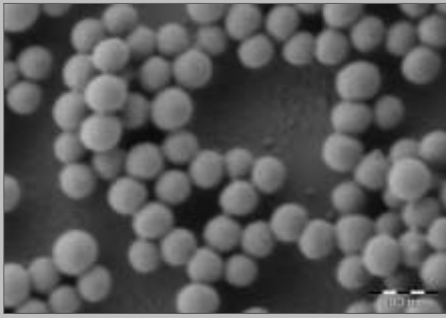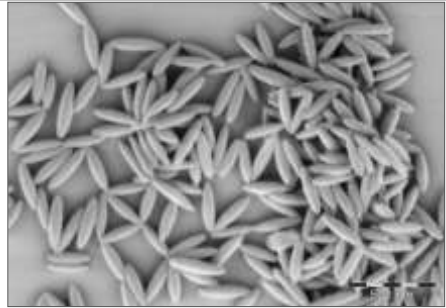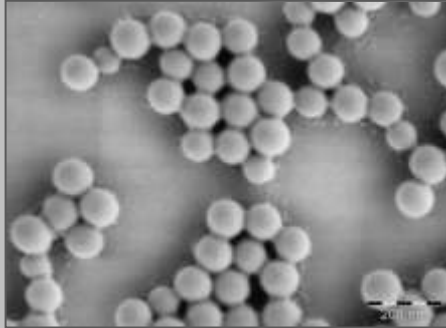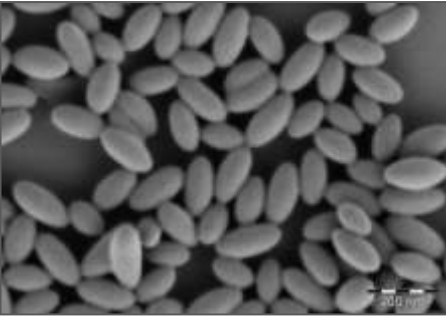
6.1.2 Optimization of particle recovery.

Parallel to the fluorescence analysis that has been described, it was necessary to improve additional aspects in the generation of anisotropic particles that are appropriate for uptake experiments in cells. Both an adequate final solid content and stability in water as a continuous phase are essential for this purpose. Firstly, the "oven stretching method" (b, section 5.1.1) made it possible to manipulate relatively larger films as by the "manual stretching in oil bath" (a, section 5.1.1) and therefore obtain a reasonable amount of material in the end of the process.

Concerning the PVA matrix removal, it was observed that the heating step (1 h at 70 °C) after dissolving the films in isopropanol/water solution had a noticeable effect on the characteristics of several of the tested dispersions. Hence, the particle dispersion CH266 was examined with Fluorescent Correlation Spectroscopy (FCS) and Scanning Electron Microscopy (SEM) after the cleaning process with and without the heating step (Table 4). Although 70 °C is still below the T_g of polystyrene (95-100 °C), SEM images showed a significant modification in particle shape. Particles lose the pre-established 4:1 aspect ratio (LF8_B, Table 4) as they tend to recover the energetically favorable spherical geometry. It is clear that the T_g value of PS is modified by the other components of the particles (e.g. styrene sulfonate and the polymerizable dye). Also, this finding regarding the heating step could have a potential use for modifying particle aspect ratio posterior to film stretching. This possibility should be anyhow tested with controlled parameters.

Additionally, FCS measurements showed higher aggregation for samples that underwent the heating step. This is recognized by occasional notably strong peaks during the FCS measurement, which deviate from the overall behavior of the curve. For the former reasons, the 1 h - 70 °C heating step was omitted in the preparation of the final samples, which were characterized and used for cell experiments. The appearance of these samples is shown in figure 19.

Table 4. Sample treatment for evaluation of heating effect after dissolving PVA matrix during particle recovery.

Sample	1h, 70°C heating step after dissolving film	SEM Image
LFK8+T_A (treated control)	No	
LF8_A	No	
LFK8+T_B (treated control)	Yes	
LF8_B	Yes	

6.1.3 Characterization: Size

The mean hydrodynamic diameter of spherical particles was larger in treated particles, although the difference is within the standard deviation of the measurements. This is also the case for the direct diameter measurements on SEM images (Table 5). The increase in size is attributed mainly to the PVA residues present after the film and cleaning process. The presented values correspond to the intensity weighed mean applying a Gaussian distribution. Additional values (number and volume weighed as well as a Nicomp Distribution) are shown in Appendix 3. Regarding ellipsoid particles, the average aspect ratio (3.62 ± 0.57) (Table 5) is lower than the pre-established value (4). This was expected for the oven
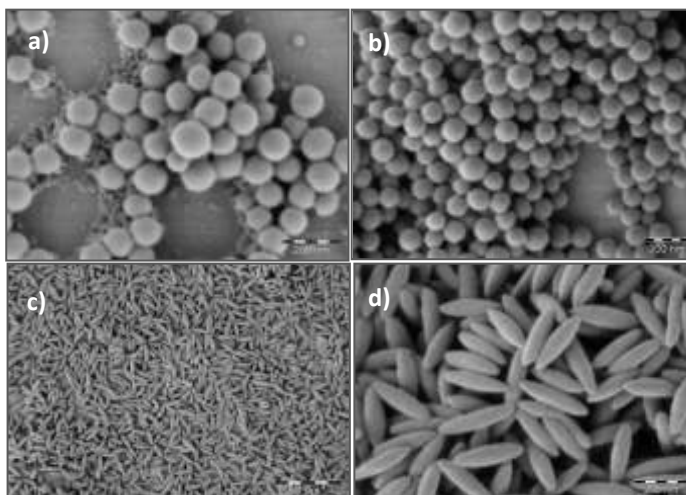
Figure 19. Isotropic and anisotropic polystyrene nanoparticles functionalized with sulfonate groups and labeled with Bodipy 2, used for cell experiments. a) Original particles CH266, corresponding to LFK8. b) Treated, unstretched particles LFK8+T_C. c) Treated, stretched particles LF8_C. d) Zoom on treated, stretched particles LF8_C.

stretching method, since the films were removed from the oven just a few seconds after elongation in order to avoid longer exposure to the high temperature. Therefore, the film experienced a slight contraction that contributed to such aspect ratio reduction.

Table 5. Particle size measured by means of Dynamic Light Scattering and directly on Scanning Electron Microscopy images.

Method	Spherical not treated	Spherical treated	Ellipsoid treated		
	Diameter (nm)	Diameter (nm)	Length (nm)	Width (nm)	Aspect Ratio
SEM	100 ± 15	105 ± 16	245 ± 37	68 ± 9	3.62 ± 0.57
DLS (D_z)	127 ± 18	137 ± 53	-	-	-

6.1.4 Characterization: charge and functionalization

Part of the original CH266 dispersion was submitted to dialysis in order to remove surfactant (SDS) and residual components from the miniemulsion synthesis. Sulfur quantification by means of ICP-MS at different times during this process provided information about the rate and extent at which sulfur-containing components (SDS and free SSNa) can be removed for this particular
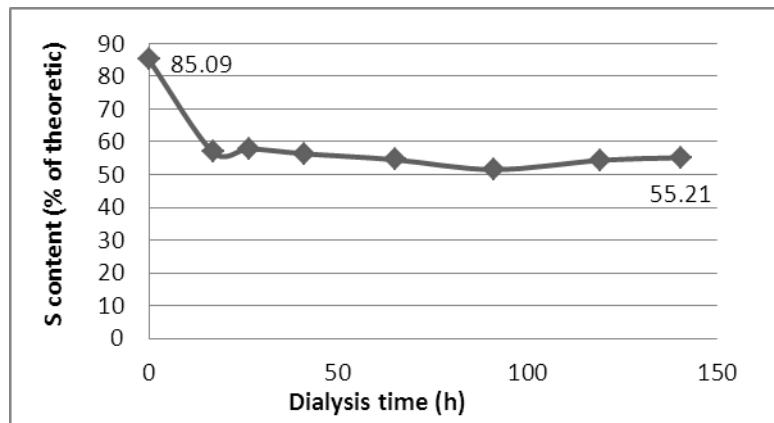
Figure 20. Sulfur content in CH266 particles measured with Inductively Coupled Plasma mass spectroscopy for different dialysis times from 0 to 145 h.

system. In conjunction with Particle Charge Detector (PCD) measurements and NMR analysis, information about the amount of charged groups associated to the particles and the presence of free charged species in the original CH266 dispersion was obtained. Precise quantification of the amount of charged groups due to effectively polymerized SSNa is nevertheless hindered by the presence of SDS (also containing negatively charged sulfur groups) and the difficulty to differentiate between these two with the available methods. According to the weighed amounts of each component for the miniemulsion synthesis (Table 2), from the total amount of sulfur theoretically 10.41% should be contributed by SDS (surfactant) and 89.59% by SSNa (comonomer).

The 85% initial sulfur content value in the non-dialyzed sample (Fig. 20) could be explained by several factors additional to a typical 5% error for ICP measurements in the applied conditions. It is important to note that the sample used for characterization and cell experiments corresponds to the dispersion *without* the coagulate present after centrifugation of the original (not dialyzed) miniemulsion product. The presence of coagulate after centrifugation suggests that rests of the sulfur containing components of the initial miniemulsion could precipitate and therefore, a fraction of these might be absent in the used sample. Also, precipitation of the different components might alter the relative amount of sulfur-containing compounds in relation to the total solid content in the sample used for characterization (without coagulate). This could be a source of error in the sulfur content calculation from the total solid content measured.

As shown in figure 20, it was possible to remove 30% of sulfur-containing material in the analyzed dispersion, including fractions of both SDS and SSNa. It is possible to recognize the removal of free unpolymerized SSNa in the ^{1}H-NMR spectra (dissolved in DMSO) of non-dialyzed and dialyzed sample, using styrene in DMSO as reference. The shifted signals with respect to the styrene protons correspond to SSNa protons. These are recognizable in the not dialyzed sample and absent in the dialyzed probe, where only the signals from polymerized styrene and styrene sulfonate are present. Additionally, it was possible to confirm that such signals were correctly attributed to styrene sulfonate (and not styrene) protons because they were absent in the spectra for both dialyzed and non-dialyzed samples in chloroform, where styrene is highly soluble and styrene sulfonate insoluble (Fig. 21). Furthermore, PCD measurements show

reduction in the number of charged groups after dialysis of the CH266 dispersion (Table 6). This is in agreement to the mentioned removal of SDS and SSNa and it indicates presence of unpolymerized SSNa in the dispersions used for film stretching and cell experiments. This fact could be relevant on interaction with cells as will be discussed in section 6.2.
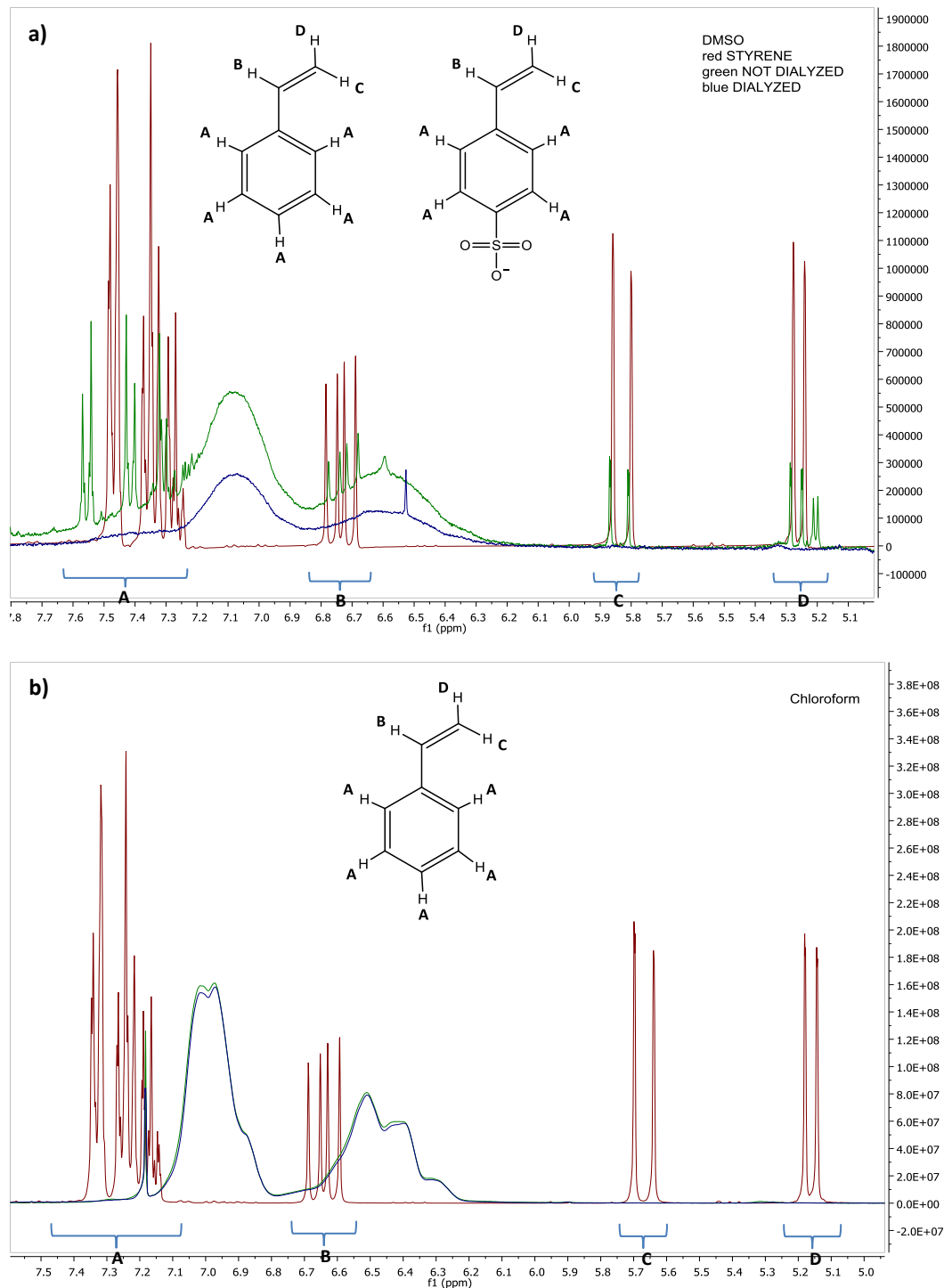
Figure 21. Liquid ¹H-NMR spectra of not dialyzed (green), dialyzed (blue) CH266 particles and styrene (red) as reference. A) In DMSO as solvent. B) In chloroform as solvent.

Table 6. Particle Charge Detector measurements for not dialyzed and dialyzed CH266 dispersion.

CH266 Sample	charges/g	groups/particle	groups/nm^2
Not dialyzed	5.68E+19	6.07E+04	1.24
Dialyzed	4.23E+19	4.52E+04	0.92

6.2 Particle uptake in MSCs

6.2.1 Particle toxicity

Cell vitality evaluated after particle addition to the seeded cells for different uptake times (1, 20 and 48 h) as well as different particle concentrations (9.4; 18.8; 37.5; 75; 150 and 300 µg/mL) showed that none of the particles (spherical not treated, spherical treated, ellipsoid treated) were toxic at any of the tested conditions. In every case at least 98% of the gated cells were still alive and no significant differences were identified among the evaluated conditions or the three different particle types (Appendix 2).

6.2.2 Influence of shape in particle uptake: qualitative assessment

6.2.2.1 Confocal Laser Scanning Microscopy (CLSM)

CLSM images confirm that particles are effectively internalized by the MSCs (Fig. 22). There are also aggregates around and on the surface of the cells, which should be considered. However, it is difficult to assure that several pictures will be representative for the whole cell population. Using a qualitative method to confirm particle internalization is in any case indispensable, since Flow Cytometry does not clearly differentiate between particles on the surface or inside the cell. Also, it is useful to revise a healthy cell appearance and the presence of single particles, which is the case in these results.
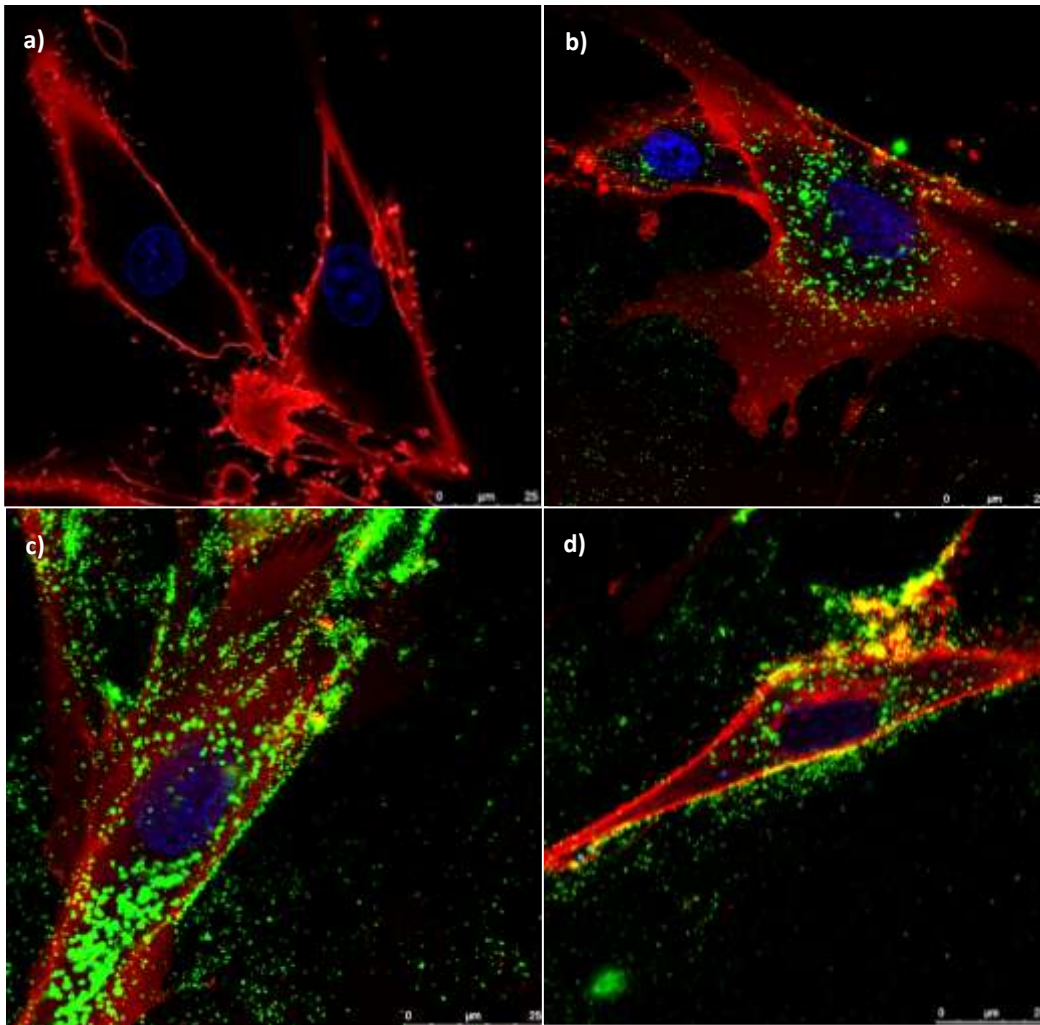
Figure 22. CLSM Images of MSCs after 20 h particle uptake at a concentration of 150 µg/mL. Particles are labeled green, the cell nucleus blue and the cell membrane red. a) Negative control, b) Spherical untreated particles (LFK8), c) Spherical treated particles (LFK8+T), d) Ellipsoid treated particles (LF8)

6.2.2.2 Scanning Electron Microscopy (SEM)

By means of SEM it was possible to recognize both situations on the cell surface: aggregated particles, as well as single particles associated to the cell membrane (Fig. 23). This was the case for the three types of particles. Entanglement by microvilli of the MSCs was also observed. Regarding aggregation, it is possible that serum proteins in the cell culture medium play a role. This will be discussed further along with the quantitative assessment of particle uptake. For ellipsoids particles both laying with their long axis parallel to the cell membrane (Fig. 24 b and d) and standing perpendicular to it (Fig. 24 c and e) were observed. The first of these situations was found more often. However, according to the established hypothesis (section 4), it could be argued that after 20 h the particles that still remain on the surface are those laying parallel to it, whereas those in perpendicular position have been taken up to a major extent. All the results mentioned above correspond to the set of particles LFK8, LFK8+T and LF8 (Table 1) after 20 h of particle addition. Additionally, micrographs of particles LF2 (Table 1) after 20 h are shown (Fig. 24 e and f). Once more, a concrete behavior or tendency cannot be defined based solely on these observations.
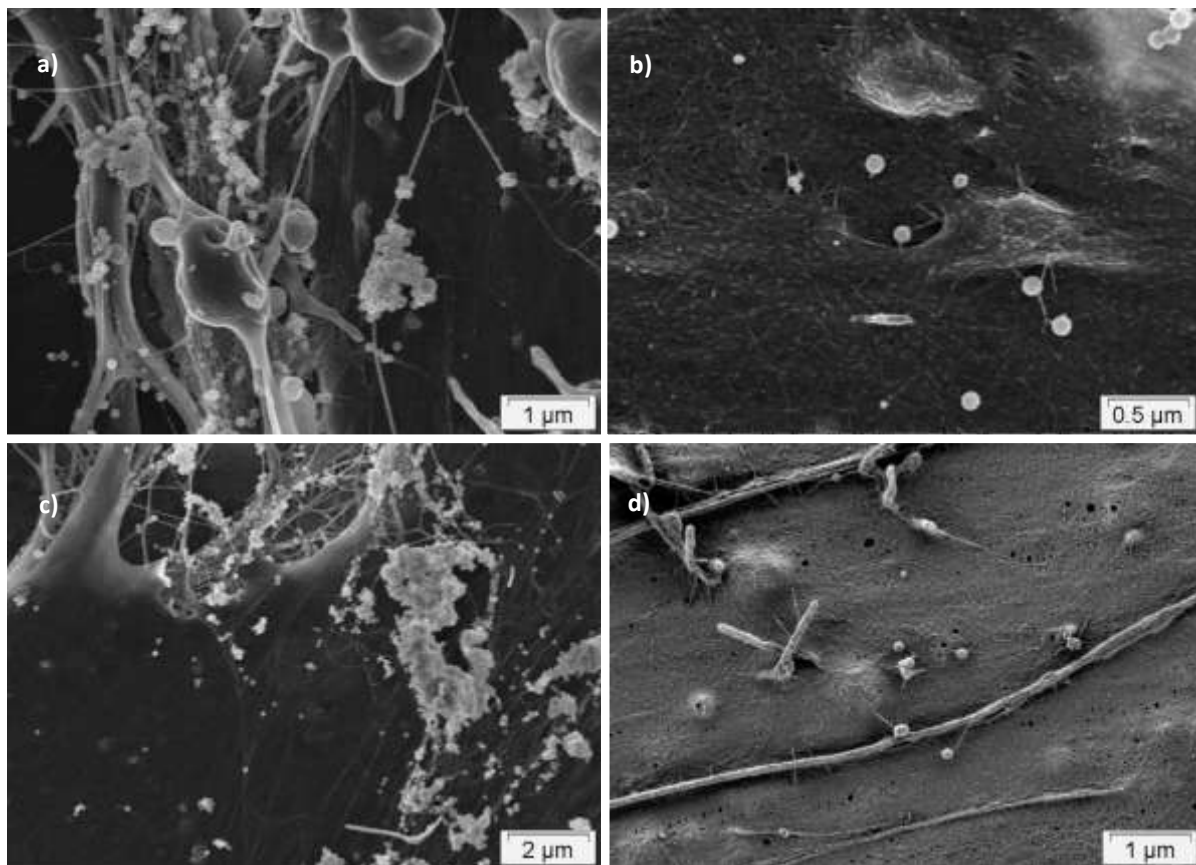
Figure 23. SEM micrographs of MSCs after 20 h of spherical particle addition at a concentration of 150 µg/mL. a) and b) not treated (LFK8). c) and d) treated (LFK8+T).

6.2.2.3 Transmission Electron Microscopy
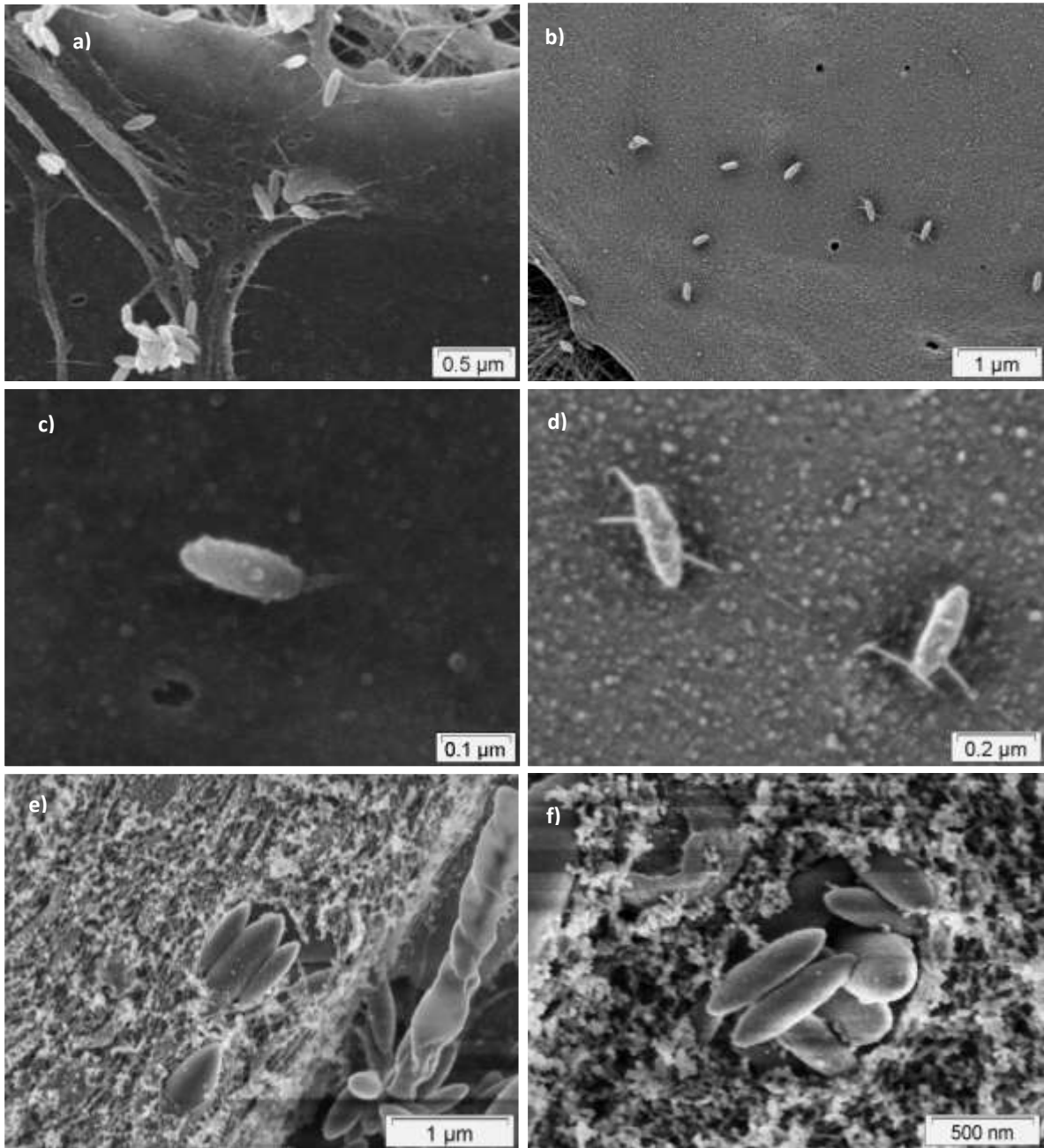
Figure 24. SEM micrographs of MSCs after 20h of ellipsoidal particle addition at a concentration of 150 µg/mL. a) to d) correspond to LF8 ; e) and f) correspond to LF2.

TEM micrographs after 20 h of particle uptake in MSCs show effective internalization in vesicles for the three types of particles (spherical not treated, spherical treated and ellipsoid treated). In most cases, several particles are observed inside each vesicle (Fig. 25 and 26).
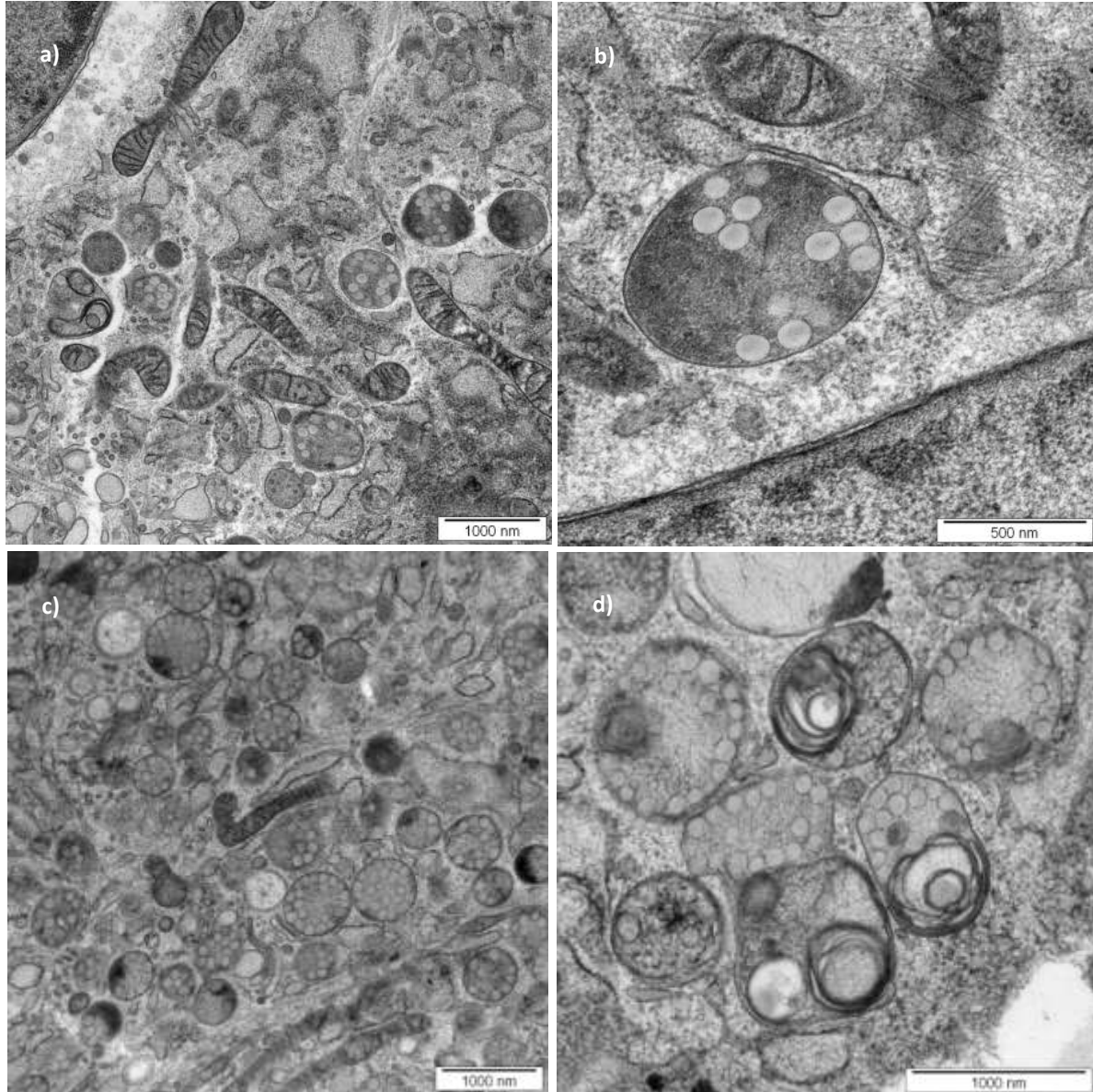
Figure 25. TEM micrographs of MSCs after 20h uptake of spherical particles at a concentration of 150 µg/mL. a) and b) not treated. c) and d) treated.
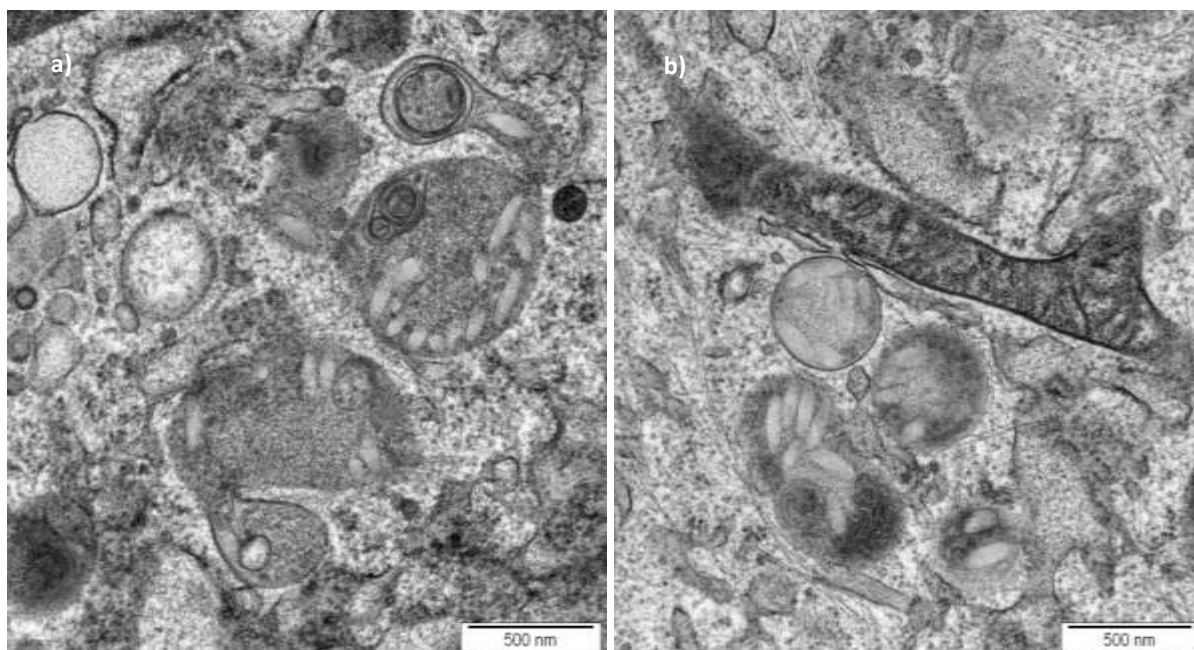
Figure 26. TEM micrographs of MSCs after 20h uptake of ellipsoid, treated particles at a concentration of 150 µg/mL.

6.2.3 Influence of shape in particle uptake: quantitative assessment

The general uptake behavior observed for the three types of particles is represented in figure 27. Regarding the effect of shape, that is, comparing spherical treated vs. ellipsoid treated, the first of these show approximately twice as much uptake as non-spherical particles for both concentrations. The significance of this difference is confirmed with 99% certainty (Table 7). This is in accordance to the predicted outcome (see section 4.2), which suggested that particle orientation would influence the probability of uptake. Considering that part of the ellipsoidal particle population will lay with the long axis parallel to the cell membrane and will therefore have a lower probability to be internalized [4, 5], the overall probability of internalization for the whole set of particles will be inferior in comparison to a complete set of spherical, isotropic particles. It is
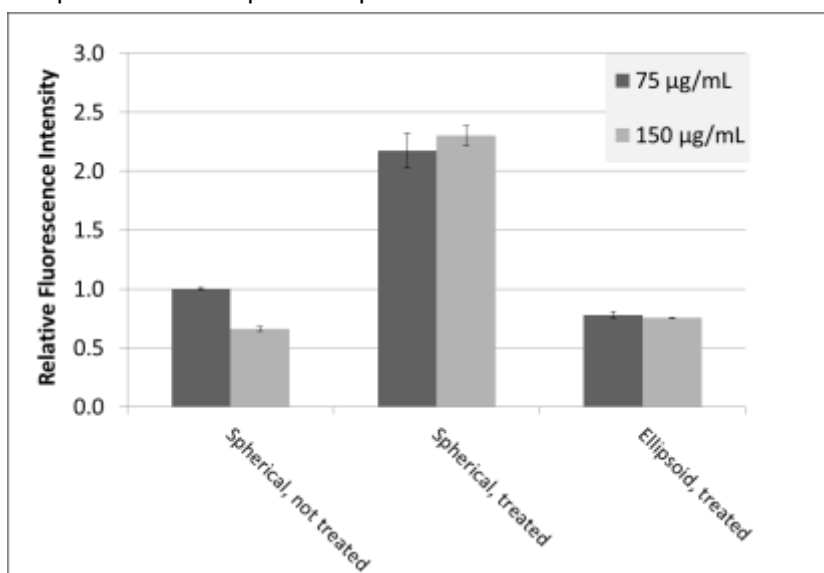
Figure 27. Particle uptake by MSCs after 20 hours at 75 and 150 µg/mL particle concentrations. Fluorescence intensity values are normalized relative to an arbitrary reference (spherical, not treated; 75 µg/mL). Error bars correspond to the standard deviation of 2 replicas, each covering at least 19,000 counts in flow cytometry.

worth to mention that nevertheless, ellipsoid particles do present internalization and are not toxic. The fact that spherical particles of the same volume and surface chemistry characteristics are preferred over ellipsoids could be considered a desirable result in specific contexts. It has been proven that cells effectively take up a wide variety of nanoparticles [1, 2, 4, 5, 7, 8, 14, 17, 19, 22, 39, 48] and therefore, it could be useful to identify a parameter that permits avoiding unspecific uptake. This is a potential tool for refining targeted delivery of drugs, genetic material or any other molecule that should be specifically directed. Once the probability of unspecific uptake or undesired phagocytosis as immunological response is reduced, the incorporation of a specific ligand could then enhance successful targeting. Work done by Champion and Mitragotri shows a related example for such outlook. They have used PS rods produced also by the film stretching method in order to inhibit phagocytosis [31]. Additionally, it has been suggested that internalization by receptor-mediated endocytosis should be attained with the incorporation of sufficient ligand densities on high curvature rims of a particle (e.g. end points of a rod) [4]. These assertions imply that an efficient specific delivery avoiding phagocytosis previous to encountering the target would be possible.

Additionally, it is noteworthy that the stretching, cleaning and recovery treatment has an effect on particle uptake. It was observed that for the same shape (spherical) treated particles are taken up to a higher degree in comparison to the not treated spheres ($p < 0.01$) (Fig. 26, Table 7). It is also worth mentioning that uptake was higher for the lower concentration tested (75 µg/mL) than for the higher (150 µg/mL) only in the case of spherical, not treated particles ($p < 0.01$) (Table 7). In order to investigate the observed differences, further experiments varying time of particle uptake and particle concentration were carried out.

Table 7. Results of two tail t-Student tests analyzing differences between means and thus evaluating the influence of particle treatment, shape and concentration. The null hypothesis corresponds to $|\mu_A - \mu_B| = 0$ and $\alpha = 0.01$ in every case.

Evaluated factor	Compared particle types (A vs. B)				
	A	Particle concentration (µg/mL)	B	Particle concentration (µg/mL)	p value
Treatment	Spherical treated	75	Spherical not treated	75	0.00328
	Spherical treated	150	Spherical not treated	150	0.00045
Shape	Ellipsoidal treated	75	Spherical treated	75	0.00080
	Ellipsoidal treated	150	Spherical treated	150	0.00180
Concentration	Spherical not treated	75	Spherical not treated	150	3.64E-09
	Spherical treated	75	Spherical treated	150	0.52079
	Ellipsoidal treated	75	Ellipsoidal treated	150	0.54772

6.2.3.1 Differential uptake in time

For every uptake time tested (from 1 to 48 hours) spherical treated particles presented once again a higher uptake in comparison to ellipsoidal particles (Fig. 28). Also, treated spherical particles were taken up to a higher extent than spherical not treated particles. This situation was maintained for all the evaluated uptake times. Furthermore, saturation was not reached even after 48 h of particle uptake while several studies of polymeric nanoparticle uptake in HeLas and MSCs report saturation or only minor difference after 20 hours at a 75 µg/mL particle concentration [1, 2, 17].
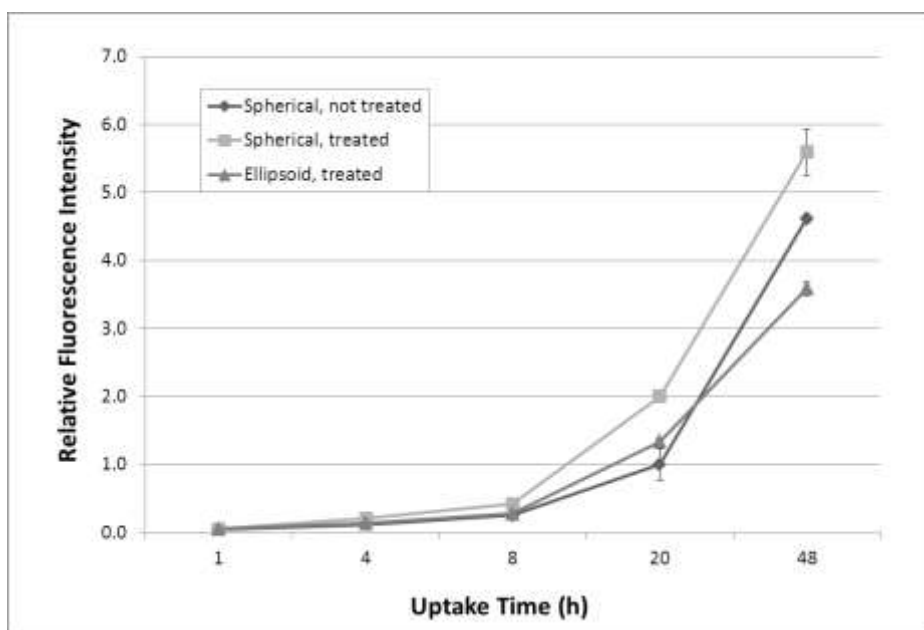
Figure 28. Particle (spherical untreated, spherical treated and ellipsoid treated) uptake by MSCs at different times after particle addition. Fluorescence intensity values are normalized relative to an arbitrary reference (spherical, not treated; 75 µg/mL). Error bars correspond to standard deviation of 2 replicas, each covering at least 5,000 counts in flow cytometry.

6.2.3.2 Uptake varying particle concentration

The outcome of the previously evaluated conditions (20 h; 75 and 150 µg/mL) was once more confirmed within the range of concentrations tested. Considering the whole series of concentrations, several noteworthy tendencies were found. First of all spherical treated particles present a higher uptake for all the tested concentrations in comparison to ellipsoidal particles (Fig. 29). Also, saturation is reached after 150 µg/mL for both treated particles regardless of shape. A different tendency was found for not treated particles, observing a decrease in uptake for concentrations of 75 µg/mL and higher. For concentrations above 18.8 µg/mL the uptake of treated spherical particles is greater in comparison to not treated (Fig. 29). These differences regarding treatment could be attributed to several factors. One of the major differences that may have an influence is the presence of PVA residues on treated particles. Other important features that could cause the observed dissimilarity are the presence of surfactant (SDS) in the not treated sample, as well as free unpolymerized sulfonated molecules (SSNa) and/or any water soluble homopolymers that are not integrated in the particles. These substances, which could be partially removed during the recovery and cleaning process on treated particles, could interfere directly or indirectly in the uptake of not treated particles. Especially in the case of charged species there can be

interaction with serum proteins in the cell culture medium that favor coagulation [1, 7]. This is particularly relevant in the case of experiments in MSCs because the cell culture medium used for these contains a relatively high amount of Fetal Calf Serum (FCS), i.e. 20%. In order to further investigate the possible causes, an additional experiment to test the effect of PVA on particle uptake was proposed, as described in the following section.
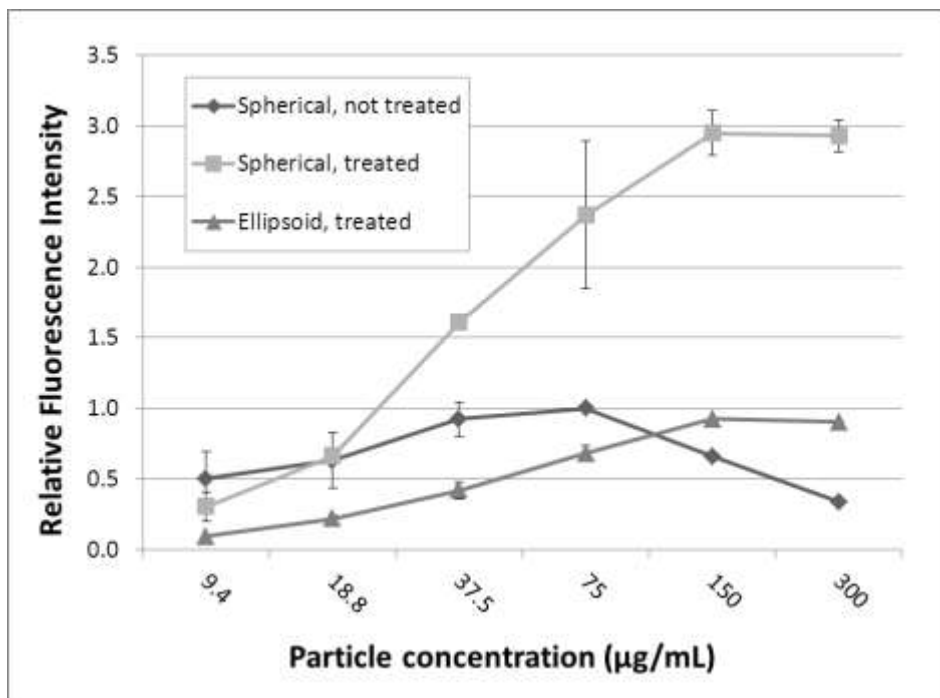

Figure 29. Particle uptake by MSCs at different concentrations for spherical untreated, spherical treated and ellipsoid treated nanoparticles. Fluorescence intensity values are normalized relative to an arbitrary reference (spherical, not treated; 75 µg/mL). Error bars correspond to standard deviation of 2 replicas, each covering at least 10,000 counts in flow cytometry.

6.2.4 Effect of treatment on particle uptake

After leaving spherical not treated particles overnight in PVA/water solutions of different concentrations and adding these samples to MSCs, it was possible to confirm that PVA is not causing the difference in uptake observed in the previous results. Particle uptake decreased with increasing PVA concentration (Fig. 30), contrary to the expected tendency if PVA residues were causing the higher uptake in treated particles. Also, the particle hydrodynamic radius increased with increasing PVA concentration, suggesting adsorption of PVA (Table 8). Eliminating the possibility of PVA as a cause for the difference in uptake of treated vs. not treated particles, the presence of surfactant and free SSNa or its homopolymer are considered to be likely causes. It is worth mentioning that interaction with sulfonate groups on polystyrene nanoparticles has been observed for specific positively charged proteins [49]. Moreover, agglomeration with serum proteins in the cell culture medium has been suggested for particles functionalized with amino groups, showing higher coagulation with increasing amount of surface charge [7]. Another study on serum protein influence on particle surface chemistry showed that, in iron magnetic particles functionalized with silanes bearing different functional groups (e.g. PEG, amino and carboxy groups), protein adsorption on the particle surface was recognized and it had a notable effect on uptake

by human cancer cells [50]. All these observations indicate that it is necessary to further investigate the interaction of serum proteins with the sulfonated particle dispersions containing ionic surfactant and free sulfonated monomer or homopolymer, in order to get a precise understanding of this outcome. Evaluation of particle uptake in MSCs for dialyzed not treated spherical particles, where a great amount of surfactant and free SSNa has been removed (Fig. 20) and the amount of charged groups on the particles has decreased (Table 6), could provide an interesting insight on the influence of these substances on particle uptake. This is a relevant inquiry, not only for understanding the effects of the stretching method applied on particle characteristics, but also for general aspects relevant to nanoparticle uptake in cells.
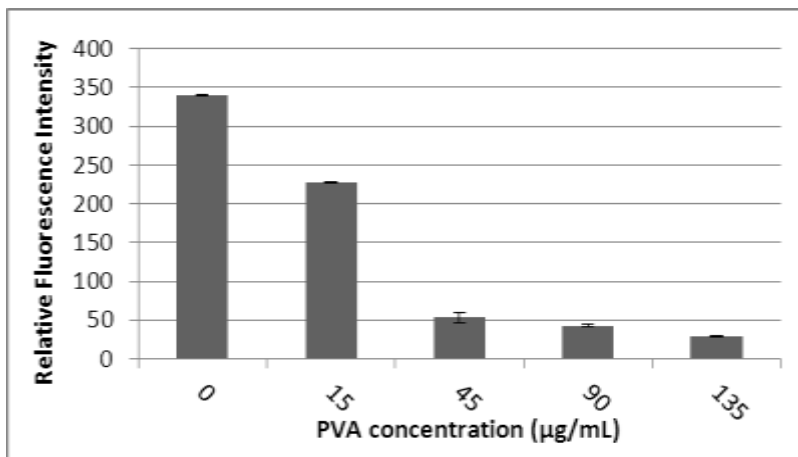
Figure 30. Uptake of spherical particles previously dispersed in PVA solutions of different concentrations, tested in MSCs for a 20 h period and 75 µg/mL particle concentration (calculated according to the solid content of the original dispersion) in every case. Each experiment was done by duplicate and error bars correspond to standard deviation.

Table 8. FCS analysis for spherical not treated particles dispersed in PVA/water solutions of different concentrations.

PVA (µg/mL)	Hydrodynamic Radius* (nm)	Measured particle concentration (nM)	Fluorescence (Counts/particle [kHz])
0	52	2.1	156 ± 23
15	61	1.7	205 ± 31
45	79	1.7	205 ± 31
90	87	2	218 ± 33
135	97	2	240 ± 36

* Not considered as exact absolute values but appropriate relative values (measured with the same calibration and under the same conditions).

7. CONCLUSIONS AND PERSPECTIVES

The production and characterization of ellipsoidal fluorescently labeled polystyrene nanoparticles together with the corresponding spherical reference particles was accomplished. Using both qualitative and quantitative methods it was possible to assess the uptake of these particles in human mesenchymal stem cells and evaluate the influence of ellipsoidal shape on uptake. None of the tested particles were toxic in any of the evaluated conditions. In accordance to the proposed hypothesis, ellipsoidal particles where taken up by MSCs to a lower extent than the reference spherical particles. This result is consistent when recalling that ellipsoids laying with the long axis parallel to the cell surface will not be easily internalized. Furthermore, it was recognized that the treatment applied for particle stretching and recovery has an influence on particle characteristics relevant for uptake by cells. Spherical treated particles presented a higher uptake than spherical not treated particles. Additionally, the uptake of not treated particles showed an unusual uptake behavior at greater particle concentrations. Instead of the typical saturation plateau, above 75 µg/mL there is a decrease in uptake. This result, together with the higher uptake of treated particles is not related to PVA residues on the surface of treated particles. It is likely that ionic surfactant (SDS), free unpolymerized comonomer (SSNa) and homopolymer present in the not treated particle dispersion are having a direct or indirect effect on uptake. Interaction with serum proteins in the cell culture medium is a possible explanation and should be investigated in detail. Further questions on mechanism variations for different particle shapes, dependence on cell type and variation on surface charge, size and aspect ratio of non-spherical particles could also offer interesting perspectives. As to applications, the present study contributes in the development of versatile tools in biological research as a model system for toxicology, immunology, virology and biomedicine. It could also be useful in promising practical applications such as delivery of DNA, drugs or specific molecules in different cell types, such as human stem cells.

8. AKNOWLEDGEMENTS

9. APPENDICES

### Appendix 1. Characteristics of all tested particles.

| ORIGINAL	LABEL	MONOMER	SURFACE FUNCT. (Comonomer)	FLUORESCENT DYE	DYE (% rel. to monomer)	SURFACTANT	INITIATOR	HYDRODYNAMIC DIAMETER (nm)	PARTICLES /PVA IN FILM (wt%)	STRETCH. METHOD	DISPERSABLE AFTER STRETCH.	SYNTH. BY
AM-ASS5-2PM	LF-K1	styrene	-	PMI		SDS	V59		-	-	no	Anna Musyanovych
	LF-1	styrene	-	PMI	0.05	SDS	V59		10	a		
DC63	LF-K2	styrene	-	PMI	0.05	LutensolAT50	KPS	390	-	-	low	Daniel Crespy
	LF-K2-T	styrene	-	PMI	0.05	LutensolAT50	KPS		10	-		
	LF-K2+T	styrene	-	PMI	0.05	LutensolAT50	KPS		10	a		
	LF-2	styrene	-	PMI	0.05	LutensolAT50	KPS		10	a		
DC64	LF-K3	styrene	-	PMI	0.05	Sodium Dodecylbenzyl sulfonate	KPS		-	-	low	Daniel Crespy
	LF-3	styrene	-	PMI	0.05	Sodium Dodecylbenzyl sulfonate	KPS		10	a		
DC65	LF-K4	styrene	-	PMI	0.05	LutensolAT50	KPS			-	low	Daniel Crespy
	LF-4	styrene	-	PMI	0.05	LutensolAT50	KPS		10	a		
AM-NSC-N1	LF-K5	styrene	$-NH_3^+$ (AEMH, 5%)	N1	0.07	CTMA-Cl	V59	164	-	-	low	Anna Musyanovych
	LF-K5+T	styrene	$-NH_3^+$ (AEMH, 5%)	N1	0.07	CTMA-Cl	V59		10	a		
	LF-5	styrene	$-NH_3^+$ (AEMH, 5%)	N1	0.07	CTMA-Cl	V59		10	a		
CH237	LF-K6	Methyl methacrylate	-	Bodipy 1	1	SDS	V59			-	low	Christoph Hauser
	LF-K6+T	Methyl methacrylate	-	Bodipy 1	1	SDS	V59		10	a		
	LF-6	Methyl methacrylate	-	Bodipy 1	1	SDS	V59		10	a		
AM-SC-Pdief	LF-K7	styrene	-	PDI	0.07	CTMA-Cl	V59		-	-	no	Anna Musyanovych
	LF-K7+T	styrene	-	PDI	0.07	CTMA-Cl	V59		5	a		
	LF-7A	styrene	-	PDI	0.07	CTMA-Cl	V59		5	a		
	LF-7B	styrene	-	PDI	0.07	CTMA-Cl	V59		5	a		
CH266	LF-K8	styrene	$-SO_3^-$ (SS, 3%)	Bodipy 2	0.5	SDS	V59	127	-	-	yes	Christoph Hauser
	LF-K8+T_A	styrene	$-SO_3^-$ (SS, 3%)	Bodipy 2	0.5	SDS	V59		8	b		
	LF-8_A	styrene	$-SO_3^-$ (SS, 3%)	Bodipy 2	0.5	SDS	V59		8	b		
	LF-K8+T_B	styrene	$-SO_3^-$ (SS, 3%)	Bodipy 2	0.5	SDS	V59		8	b		
	LF-8_B	styrene	$-SO_3^-$ (SS, 3%)	Bodipy 2	0.5	SDS	V59		8	b		
	LF-K8+T_C	styrene	$-SO_3^-$ (SS, 3%)	Bodipy 2	0.5	SDS	V59		8	b		
	LF-8_C	styrene	$-SO_3^-$ (SS, 3%)	Bodipy 2	0.5	SDS	V59		8	b		
CH257-2	LF-K9	styrene	-	Bodipy 2	0.5	SDS	V59	140	-	-	low	Christoph Hauser
	LF-K9+T	styrene	-	Bodipy 2		SDS	V59		8	b		
	LF-9	styrene	-	Bodipy 2		SDS	V59		8	b		
CH267	LF-K10	styrene	$-SO_3^-$ (SS, 3%)	Bodipy 2	0.25	SDS	V59	115	-	-	-	Christoph Hauser

Appendix 2. MSC vitality evaluated with 7AAD.

Cell (MSC) vitality evaluated with 7AAD for different particle concentrations. Particle uptake time was 20 h for every case.
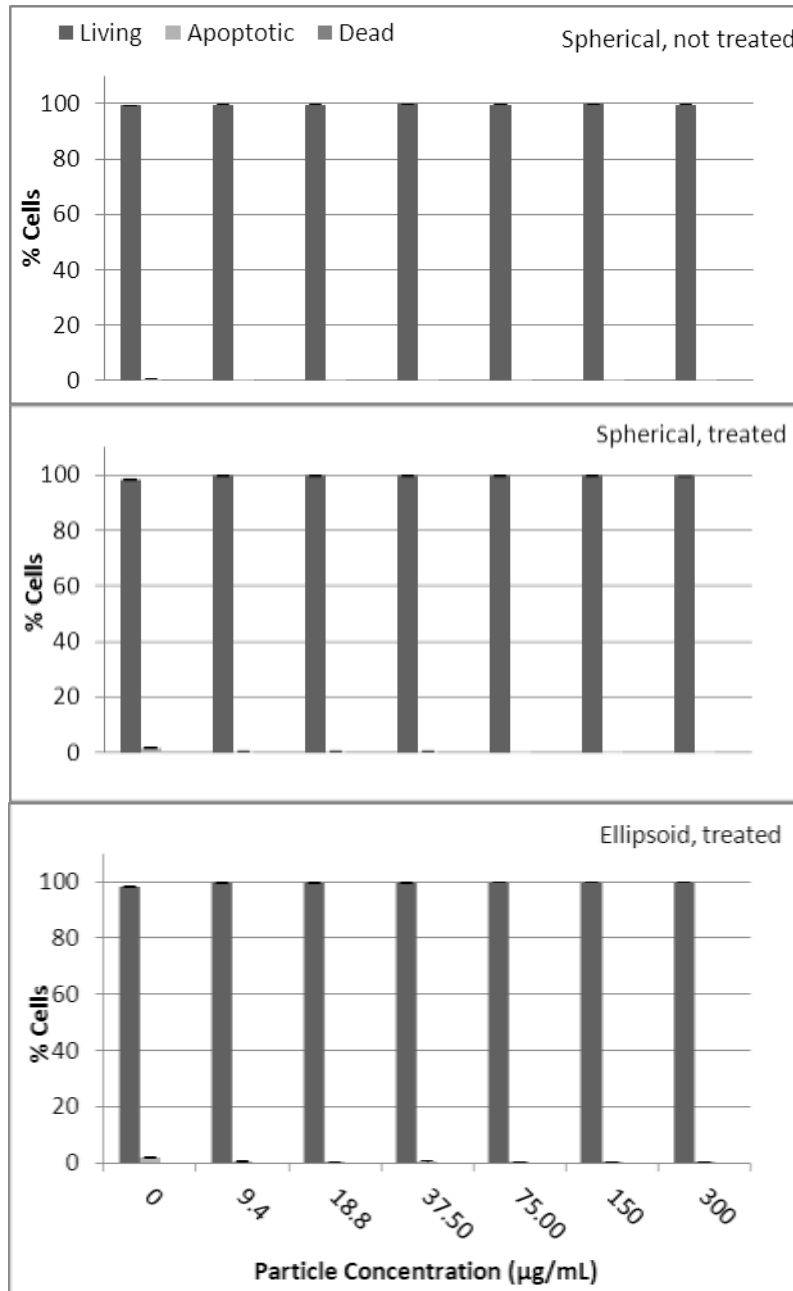
Cell (MSC) vitality evaluated with 7AAD for different particle uptake periods. Particle concentration was 75 μg/mL for every case.
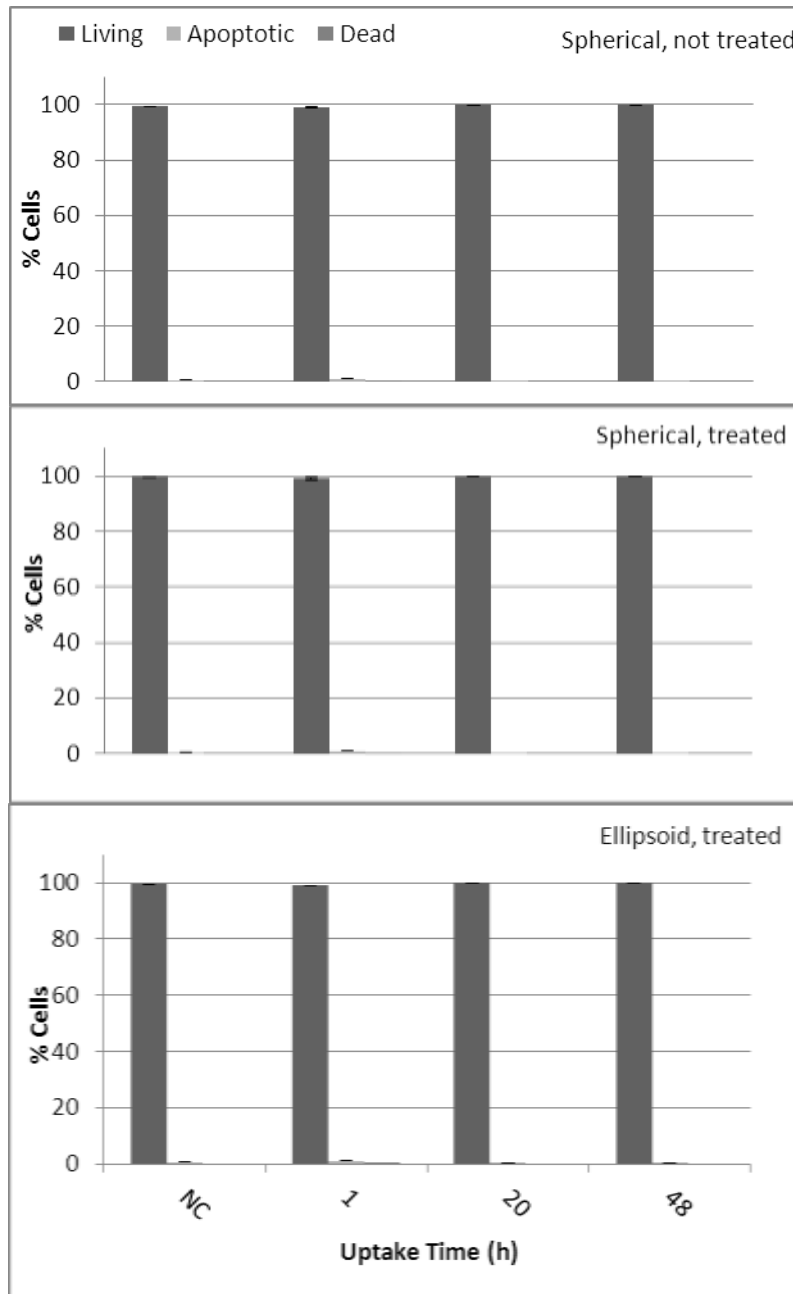
Cell (MSC) vitality evaluated with 7AAD for particles in PVA/water solutions of different concentrations. Particle concentration was 75 µg/mL and uptake time 20 h for every case.
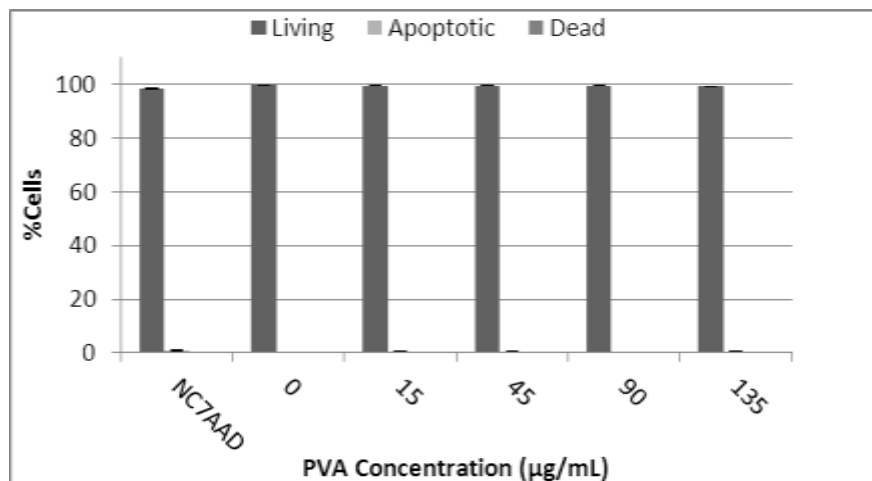
Appendix 3.

Hydrodynamic diameter of spherical not treated and treated particles measured by means of DLS.

SAMPLE	Hydrodynamic Diameter according to Gaussian Distribution (nm)				Hydrodynamic Diameter according to Nicomp Distribution (nm)			
	Intensity Weighting	Std. Dev	Number Weighting	Std. Dev	Intensity Weighting	Percent included	Number Weighting	Percent included
LFK8	127	18	113	16	125	100	114	100
LFK8+T	137	53	57	22	117	79.51	107	99.76

10.   LIST OF FIGURES

11. LIST OF TABLES

12. LIST OF ACRONYMS AND TECHNICAL TERMS

Name	Acronym	Description for this study
2,2'-Azobis(2-methylbutyronitrile)	V59	Oil soluble radical polymerization initiator
Acrylic acid	AA	Comonomer
Amino Ethyl Methacrylate Hydrochloride	AEMH	Comonomer
boron-dipyrromethene dye	Bodipy	Boron-dipyrromethene dye (1 or 2)
Cetryltrimethylammonium Chloride	CTMA-Cl	Surfactant
Confocal Laser Scanning Microscopy	CLSM	Analysis method
Dimethyl Sulfoxide	DMSO	Solvent
Dynamic Light Scattering	DLS	Analysis method
Fetal Calf Serum	FCS	Growth factor- containing component in cell culture media
Fluorescence Activated Cell Sorting (Flow Cytometry)	FACS	Analysis method
Fluorescence Correlation Spectroscopy	FCS	Analysis method
Human epithelial cervical cancer cell	HeLa	Cell line commonly used in cell culture studies
Human Mesenchymal Stem Cells	MSCs	Cell line used in experiments
Inductively Coupled Plasma Spectroscopy	ICP	Analysis method
N-(2,6-diisopropylphenyl)perylene-3,4-dicarbonacidimide)	PMI	Perylene dye
Particle Charge Detector	PCD	Analysis method
Poly-(ethylene glycol)	PEG	Polyether used for particle functionalization
Poly-(methyl methacrylate)	PMMA	monomer
Poly-(vinyl alcohol)	PVA	Film matrix
Polystyrene	PS	monomer
Potassium Persulfate	KPS	Water soluble radical polymerization initiator
Rhodamine 6G	Rh6G	Fluorone dye, reference in fluorescence spectroscopy
Scanning Electron Microscopy	SEM	Analysis method
Sodium Dodecyl Sulfate	SDS	Surfactant
Sodium Styrene Sulfonate	SSNa	Sulfonated copolymer
Transmission Electron Microscopy	TEM	Analysis method

13. LITERATURE

1.   Mailander, V. and K. Landfester, *Interaction of nanoparticles with cells.* Biomacromolecules, 2009. **10**(9): p. 2379-400.
2.   Landfester, K., A. Musyanovych, and V. Mailänder, *From polymeric particles to multifunctional nanocapsules for biomedical applications using the miniemulsion process.* Journal of Polymer Science Part A: Polymer Chemistry, 2010. **48**(3): p. 493-515.
3.   Champion, J.A., Y.K. Katare, and S. Mitragotri, *Particle shape: A new design parameter for micro- and nanoscale drug delivery carriers.* Journal of Controlled Release, 2007. **121**(1-2): p. 3-9.
4.   Decuzzi, P. and M. Ferrari, *The Receptor-Mediated Endocytosis of Nonspherical Particles.* Biophysical Journal, 2008. **94**(10): p. 3790-3797.
5.   Decuzzi, P., et al., *Intravascular Delivery of Particulate Systems: Does Geometry Really Matter?* Pharmaceutical Research, 2009. **26**(1): p. 235-243.
6.   Zauner, W., N.A. Farrow, and A.M.R. Haines, *In vitro uptake of polystyrene microspheres: effect of particle size, cell line and cell density.* Journal of Controlled Release, 2001. **71**(1): p. 39-51.
7.   Lorenz, M.R., et al., *Uptake of functionalized, fluorescent-labeled polymeric particles in different cell lines and stem cells.* Biomaterials, 2006. **27**(14): p. 2820-2828.
8.   Dausend, J., et al., *Uptake Mechanism of Oppositely Charged Fluorescent Nanoparticles in HeLa Cells.* Macromolecular Bioscience, 2008. **8**(12): p. 1135-1143.
9.   Champion, J.A. and S. Mitragotri, *Role of target geometry in phagocytosis.* Proceedings of the National Academy of Sciences of the United States of America, 2006. **103**(13): p. 4930-4934.
10.   Chithrani, B.D., A.A. Ghazani, and W.C.W. Chan, *Determining the Size and Shape Dependence of Gold Nanoparticle Uptake into Mammalian Cells.* Nano Letters, 2006. **6**(4): p. 662-668.
11.   Gratton, S.E.A., et al., *The effect of particle design on cellular internalization pathways.* Proceedings of the National Academy of Sciences, 2008. **105**(33): p. 11613-11618.
12.   Zhang, K., et al., *Shape Effects of Nanoparticles Conjugated with Cell-Penetrating Peptides (HIV Tat PTD) on CHO Cell Uptake.* Bioconjugate Chemistry, 2008. **19**(9): p. 1880-1887.
13.   Antonietti, M. and K. Landfester, *Polyreactions in miniemulsions.* Progress in Polymer Science, 2002. **27**(4): p. 689-757.
14.   Tautzenberger, A., et al., *Effect of functionalised fluorescence-labelled nanoparticles on mesenchymal stem cell differentiation.* Biomaterials, 2010. **31**(8): p. 2064-2071.
15.   Landfester, K., *Miniemulsion polymerization and the structure of polymer and hybrid nanoparticles.* Angew Chem Int Ed Engl, 2009. **48**(25): p. 4488-507.
16.   Musyanovych, A., et al., *Effect of hydrophilic comonomer and surfactant type on the colloidal stability and size distribution of carboxyl- and amino-functionalized polystyrene particles prepared by miniemulsion polymerization.* Langmuir, 2007. **23**(10): p. 5367-76.
17.   Musyanovych, A., et al., *Preparation of biodegradable polymer nanoparticles by miniemulsion technique and their cell interactions.* Macromol Biosci, 2008. **8**(2): p. 127-39.
18.   Vaihinger, D., et al., *Molecularly imprinted polymer nanospheres as synthetic affinity receptors obtained by miniemulsion polymerisation.* Macromolecular Chemistry and Physics, 2002. **203**(13): p. 1965-1973.
19.   Jiang, X., et al., *Specific Effects of Surface Amines on Polystyrene Nanoparticles in their Interactions with Mesenchymal Stem Cells.* Biomacromolecules, 2010. **11**(3): p. 748-753.
20.   Corsi, K., et al., *Mesenchymal stem cells, MG63 and HEK293 transfection using chitosan-DNA nanoparticles.* Biomaterials, 2003. **24**(7): p. 1255-1264.

21. Holzapfel, V., et al., *Preparation of Fluorescent Carboxyl and Amino Functionalized Polystyrene Particles by Miniemulsion Polymerization as Markers for Cells.* Macromolecular Chemistry and Physics, 2005. **206**(24): p. 2440-2449.

22. Lorenz, S., et al., *The Softer and More Hydrophobic the Better: Influence of the Side Chain of Polymethacrylate Nanoparticles for Cellular Uptake.* Macromolecular Bioscience, 2010. **9999**(9999): p. NA.

23. Näreoja, T., et al., *Study on nonspecificity of an immuoassay using Eu-doped polystyrene nanoparticle labels.* Journal of Immunological Methods, 2009. **345**(1-2): p. 80-89.

24. Azzi, J., et al., *Polylactide-cyclosporin A nanoparticles for targeted immunosuppression.* The FASEB journal : official publication of the Federation of American Societies for Experimental Biology, 2010. **24**(10): p. 3927-38.

25. Jayakumar, R., et al., *Chitosan conjugated DNA nanoparticles in gene therapy.* Carbohydrate Polymers, 2010. **79**(1): p. 1-8.

26. Li, Z. and L. Huang, *Sustained delivery and expression of plasmid DNA based on biodegradable polyester, poly(,-lactide-co-4-hydroxy--proline).* Journal of Controlled Release, 2004. **98**(3): p. 437-446.

27. Cohen, H., et al., *Sustained delivery and expression of DNA encapsulated in polymeric nanoparticles.* Gene Therapy, 2000. **7**(22): p. 1896-1905.

28. Patil, Y. and J. Panyam, *Polymeric nanoparticles for siRNA delivery and gene silencing.* International Journal of Pharmaceutics, 2009. **367**(1-2): p. 195-203.

29. Lares, M.R., J.J. Rossi, and D.L. Ouellet, *RNAi and small interfering RNAs in human disease therapeutic applications.* Trends in Biotechnology, 2010. **28**(11): p. 570-579.

30. Mitragotri, S., *In Drug Delivery, Shape Does Matter.* Pharmaceutical Research, 2009. **26**(1): p. 232-234.

31. Champion, J. and S. Mitragotri, *Shape Induced Inhibition of Phagocytosis of Polymer Particles.* Pharmaceutical Research, 2009. **26**(1): p. 244-249.

32. Adler, A.F. and K.W. Leong, *Emerging links between surface nanotechnology and endocytosis: Impact on nonviral gene delivery.* Nano Today. **In Press, Corrected Proof**.

33. Kirkham, M. and R.G. Parton, *Clathrin-independent endocytosis: New insights into caveolae and non-caveolar lipid raft carriers.* Biochimica et Biophysica Acta (BBA) - Molecular Cell Research, 2005. **1745**(3): p. 273-286.

34. Dendukuri, D., et al., *Controlled Synthesis of Nonspherical Microparticles Using Microfluidics.* Langmuir, 2005. **21**(6): p. 2113-2116.

35. Ho, C.C., et al., *Preparation of monodisperse ellipsoidal polystyrene particles.* Colloid & Polymer Science, 1993. **271**(5): p. 469-479.

36. Madivala, B., et al., *Exploiting particle shape in solid stabilized emulsions.* Soft Matter, 2009. **5**: p. 1717 - 1727.

37. Chung, T.-H., et al., *The effect of surface charge on the uptake and biological function of mesoporous silica nanoparticles in 3T3-L1 cells and human mesenchymal stem cells.* Biomaterials, 2007. **28**(19): p. 2959-2966.

38. Greulich, C., et al., *Studies on the biocompatibility and the interaction of silver nanoparticles with human mesenchymal stem cells (hMSCs).* Langenbecks Arch Surg, 2009. **394**(3): p. 495-502.

39. Mailänder, V., et al., *Carboxylated Superparamagnetic Iron Oxide Particles Label Cells Intracellularly Without Transfection Agents.* Molecular Imaging and Biology, 2008. **10**(3): p. 138-146.

40. Park, J.S., et al., *Non-viral gene delivery of DNA polyplexed with nanoparticles transfected into human mesenchymal stem cells.* Biomaterials, 2010. **31**(1): p. 124-132.

41.   Pittenger, M.F. and B.J. Martin, *Mesenchymal Stem Cells and Their Potential as Cardiac Therapeutics.* Circ Res, 2004. **95**(1): p. 9-20.

42.   Karolin, J., et al., *Aggregation of perylene dyes in lipid vesicles: The effect of optically active substituents.* Spectrochimica Acta Part A: Molecular and Biomolecular Spectroscopy, 1996. **52**(7): p. 747-753.

43.   Türkmen, G., S. Erten-Ela, and S. Icli, *Highly soluble perylene dyes: Synthesis, photophysical and electrochemical characterizations.* Dyes and Pigments, 2009. **83**(3): p. 297-303.

44.   Ulrich, G., R. Ziessel, and A. Harriman, *The Chemistry of Fluorescent Bodipy Dyes: Versatility Unsurpassed13.* Angewandte Chemie International Edition, 2008. **47**(7): p. 1184-1201.

45.   Landfester, K., *SYNTHESIS OF COLLOIDAL PARTICLES IN MINIEMULSIONS.* Annual Review of Materials Research, 2006. **36**(1): p. 231-279.

46.   Mueller, W., et al., *Hydrophobic Shell Loading of PB-b-PEO Vesicles.* Macromolecules, 2008. **42**(1): p. 357-361.

47.   Langhals, H., R. Ismael, and O. Yürük, *Persistent Fluorescence of Perylene Dyes by Steric Inhibition of Aggregation.* Tetrahedron, 2000. **56**(30): p. 5435-5441.

48.   Weiss, C.K., et al., *Cellular uptake behavior of unfunctionalized and functionalized PBCA particles prepared in a miniemulsion.* Macromol Biosci, 2007. **7**(7): p. 883-96.

49.   Liang, L., et al., *Interaction of Apo Cytochrome c with Sulfonated Polystyrene Nanoparticles.* Langmuir, 2004. **20**(8): p. 3333-3338.

50.   Chen, Z., et al., *Effects of Proteins from Culture Medium on Surface Property of Silanes-Functionalized Magnetic Nanoparticles.* Nanoscale Research Letters, 2009. **4**(3): p. 204-209.